An Aero Structural Study and Optimization of Modern Truss Braced Wings

a project is presented to
The Faculty of the Department of Aerospace Engineering San José State University

in partial fulfillment of the requirements for the degree
Masters of Science in Aerospace Engineering

by

Ryan K. Lee
December 2021

approved by

Dr. Maria Chierichetti
Faculty Advisor

SAN JOSÉ STATE
UNIVERSITY

Table

1. Introduction

1.1 Motivation

New emerging technologies are constantly created each year that end up solving a multitude of problems. However with increasing concerns regarding climate health and energy consumption, a trend in modern day engineering is the need to implement more fuel efficient technologies that reduce the environmental impact of high emission vehicles. With the extensive use of airliners transporting passengers around the globe, significant effort is being put forth to discover new methods to increase the efficiency of these types of aircraft. A Boeing program named the Subsonic Ultra Green Aircraft Research [1] hopes to release more efficient low emissions aircraft between 2030 and 2040 with significantly lower fuel usage than previous airline models through a variety of multi-disciplinary design changes.

Since aerodynamics play a significant factor when determining the fuel efficiency of an aircraft, a high aspect ratio low thickness to chord wing concept that would increase the aerodynamic efficiency of an aircraft is under research for future transonic airliner applications. The thinner wings allow for a reduction of transonic wave drag allowing for a reduction in wing sweep and in turn parasite drag. The increase in aspect ratio lowers the induced drag which, coupled with reduced wing thickness, drastically improves its performance. High aspect ratio wings have been incorporated in emissionless gliders for decades, however implementation in large transport aircraft such as airliners have yet to be achieved due to the increased load that the wings would need to endure. Such slim, high aspect ratio designs would elicit structural shortcomings that yield to issues with wing flex, flutter, and torsion that, unlike typical cantilever wings, must be accounted for through alternative bracing methods. These methods of structural bracing can no longer be retained inside the geometrical constraints of the wing itself due to the increased wing stress. Werner Pfenninger [2] proposed a truss braced wing configuration that incorporates a strut and jury strut bracing geometry for each wing to allow for the longer aspect ratio while retaining its structural integrity. He found that although this increase in aspect ratio yielded a weaker wing structure as a stand alone assembly, the addition of truss bracing increased

on the fully assembled system had enough strength to compensate for the weaker wing structure while retaining superior aerodynamic characteristics.

With such design yielding promising aerodynamic results, this project seeks to find the most optimal structural bracing design to support the longer and thinner wing geometries while retaining the aerodynamic, weight, strength advantages over present cantilever aircraft wings.

1.2 Literature Review

Although the concept of high aspect ratio truss braced wings has been conceptualized for the past half century, significant effort into its application in modern transonic general aviation has not begun until recently. This section is an overview of the previous research that has been accomplished in regards to the optimization of truss and strut braced wing configurations.

The first implementations in the truss braced design for transport aircraft is dated to 1953 when Hurel Dubois developed and produced eight HD-34s with a 20.2 aspect ratio. He proposed the implementation of the large aspect ratio wing with lifting truss supports. The large aspect ratio would reduce the induced drag and while the truss supports would provide the additional bracing to prevent any elicited flex. This concept was revisited in 1975 with Werner Pfenninger's truss braced wing design [2] that implemented an aspect ratio of 16.3. The wing is designed with a thinner chord as a result of the truss implementation. Claims were that the concept would weigh less than typical cantilever wing setups while retaining a superior L/D and laminar flow characteristics.

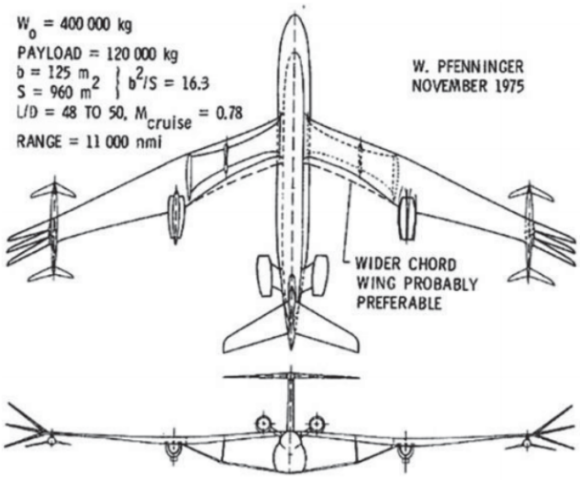

Figure 1 - Werner Pfenninger's concept of a more efficient high aspect ratio wing

Recent research regarding this subject of truss bracing concepts are designed around typical mid size regional airline bodies including the Boeing 777 and 737 with a modified T tail due the downstream aerodynamics effects of the main wing truss. Most studies revolve around this configuration's baselines such as truss placement, and wing geometry. Studies are based around the conclusions formed from parameterized algorithms that consider specific parameters ranging from geometrical to weight to fuel considerations and result in various output designs that can show the best models for specific mission goals.

Boeing partnered with Virginia Tech and NASA to run multi disciplinary optimizations on various truss braced models for the SUGAR high project [3]. These concepts were designed around a typical regional general aviation aircraft, specifically the Boeing 777-200IGW mission profile, with a 305 passenger payload, mach 0.85 cruise speed, and 7,380mi range. Initial phase I studies incorporating computational testing involved Virginia Tech's multidisciplinary design algorithm that ran iterations with varying parameters and concluded with the most optimal designs for various outputs such as fuel weight/emissions and L/D [4]. The results show that varying single strut braced configurations have a 38% reduction in fuel burn over a 900 nautical mile range with a 58% potential fuel burn savings with additional technology improvements. The best models for various parameters are pulled from the iterations to understand design

characteristics that affect these parameters [5,6]:

Optimized minimum fuel weight/emission:

- Increased span is allowed by the bracing
- Increases L/D
- Lowers induced drag
- Increased wing area
- High cruise altitude
- Decrease zero-lift drag coefficient
- Lower fuel weight and TOGW

Maximum L/D:

- Longest spans up to 250ft
- Largest aspect ratios up to 1:23
- Fuel weight in these models were higher due to increase wing weight

Phase III of the research, completed in 2019 [7], incorporated the use of dynamically scaled models which produced results that show both advantages and disadvantages with truss and strut braced designs. At mach 0.7, the strut braced wing performs favorably as a more desirable take off gross weight and fuel consumption was observed. However for transonic speeds at mach 0.8, the truss braced wing is more suitable. The additional bracing from the jury struts prevent inboard wing bending and produce a more satisfying flutter constraint.

In addition to pure bending and torsional loading, the effect of flutter is also important. Flutter occurs when a wing begins to uncontrollably oscillate due to dynamic instability. An additional paper [8] working along with Virginia Tech's SUGAR project highlighted the effects that flutter played on the truss braced wing. The MDO study created a fixed flutter constraint and focused on reducing the fuel consumption and TOGW. With a $1.15V_D$ flutter constraint, the best design resulted in a 1.5% for the medium range and 3.2% long range mission increase in TOGW. The report noted that for longer range missions, external reinforcement was required at

the inboard section of the strut where the medium range mission required reinforcement at the outboard section of the strut. With regards to fuel consumption, the medium range mission increased fuel consumption by 5% while the long range mission increased fuel consumption by 7.5% The paper notes that the aggressive increases in fuel burn make active means of flutter mitigation attractive.

Many of the struggles created by this design relate back to balance of the aerodynamic performance and the additional weight of the bracing structure. As the length of the wing increases, so does the need to add more weight and costly bracing. However, modern day composite materials that have a better strength to weight ratio make the potential for an originally heavy design become more feasible. A different computational test was conducted [9] on the truss braced configuration proposed by Boeing's SUGAR project, however a composite [0, +45, -45, 90] laminate schedule was used for the skin while aluminum alloy is used for the spar and ribs. The constraint was the strain of the materials and the flutter speed in relation to the flight envelope. The test simulated a 2.5G pull, -1G push over, and 25degree aileron deflection at mach 0.6 and 0.785.

Modeling the efficiency of the various braced configurations is a challenging concept to quantify, however recent studies claim that the usage of take off gross weight (TOGW) is an accepted quantity to indicate the life cycle cost of the aircraft. One independent study [10], that marked conclusions heavily based on the TOGW, compared configurations of a low wing cantilever, high wing cantilever, high wing strut, high wing truss design. The study is based on a 737-800 body and a controlled computation multidisciplinary study shows that the configurations with the most optimal parameters yielded increasing weight in the following order: low wing cantilever, high wing cantilever, strut, and truss. This study was very controlled as each wing configuration allowed only the wing geometry and engine placement to be optimized. Without further optimization within the truss or strut structure itself, it is observed that the addition of bracing members does not benefit the overall efficiency of the aircraft. The study notes that the configuration that has the highest L/D also is the configuration with the

highest TOGW. This is due to the large wing area that needs a larger and heavier engine to provide the thrust to carry the aircraft to the set range.

Previous literature provides insight into the risky but high potential nature of the truss braced wings. Unlike cantilever wings, the additional bracing allows for more flexibility within the wing design by allowing the wings aspect ratio to increase, however the increase in wing size brings along new issues of weight associated with the potential increase in engine size and additional bracing material. As shown in NASA's tests, a structurally and aerodynamically designed configuration does prove beneficial over cantilever wings, even with the disadvantages associated with the truss setup.

1.3 Project Proposal

The 21st century has brought on many new goals and challenges, however one of the most recognized goals is the need to reduce fuel emissions and develop more environmentally friendly methods of transportation. Boeing revealed their plans to design a transonic aircraft with large reductions in fuel emissions while increasing cruise speed as a result of various novel aerodynamic and fuel/power source modifications. This project, assigned the name Subsonic Ultra Green Aircraft Research (SUGAR) [4], hopes to release the aircraft between 2030 and 2040. One of the sub-branches of Boeing's SUGAR research, termed SUGAR High [1], relies on a Werner Pfenninger's high wing configuration [2], Fig. 1 with a geometry that has a significantly larger aspect ratio than the typical cantilever airliner wing. This larger aspect ratio yields reductions in induced drag, transonic wave drag, and overall L/D performance. This ultimately results in an aircraft that can travel at the same speed or faster than present day aircraft while consuming less fuel.

Although this configuration has its aerodynamics advantages, the slender wing design augments structural problems such as flutter, high bending, and torsional flex, resulting in large stresses. An innovative approach to improve the structural design focuses on incorporating a

support structure composed of trusses and struts between the fuselage and wing, as a method to stiffen the wing and mitigate the structural issues while still retaining advantageous aerodynamics and weight characteristics over standard cantilever unbraced wings.

1.4 Methodology

1.4.1 Description of Study

The goal of this project is to study and design a bracing structure for a modern high aspect ratio wing that is twice that of existing configurations operating in the subsonic and transonic regime. The first phase of this project focuses on existing research to determine the promising bracing concepts in terms of aeroelastic and aerostructural performance. Based on these previous findings, a baseline aircraft wing geometry will be created to allow for a uniform and controlled design study. The configurations identified in existing literature will be performed and reproduced on this baseline wing model to ensure a controlled design study is executed. Finite element analysis will then be conducted on each configuration to identify the most important parameters that contribute to and improve the structural integrity of the wing. Based on the identified factors, the next phase of the project will focus on designing a new and improved bracing concept. The following is a schematic breakdown of this projects scope:

Phase 1: Identify favorable bracing characteristics

1) Identify baseline wing structure and types of bracing structures that will be implemented
2) Based on existing information, identify bracing configurations (cantilever, strut, truss...etc) and how each configuration affects the aerostructural performance
3) Build a finite element model for each configuration and compare performance of each configuration in terms of structural efficiency and stiffness. This is used to identify specific factors and how they affect the performance of the wing

Phase 2: Create a new bracing design and perform tests and validation

1) Design a new optimized bracing configuration from data learned in phase 1

2) Perform numerical design validation and analysis through finite element analysis

1.4.2 Chapter Overview

Chapter 1

A general review of the present status regarding the development of bracing for transonic high aspect ratio wings. This review describes early concepts that started the theory of truss braced wings and notable research conducted to create production feasible brace designs.

Chapter 2

The selection for the baseline aircraft for the study to be conducted around. The primary application of these designs are for airline and transportation aircraft and a suitable aircraft for comparison is selected in the chapter.

Chapter 3

Review existing bracing design both for internal and external reinforcement

Chapter 4

Perform proven calculations to simulate the effect of aerodynamic loads on a wing type structure. This will provide a reference for continuing chapters to ensure the more advanced methods are still in line with the classical calculations

Chapter 5

Use an aerodynamically and geometrically accurate model with internal framing and ribbing to create a baseline cantilever FEA model. Based on this result the final product with external bracing will be referred back to this chapter's design to compare the improvements and disadvantages of an externally braced design.

Chapter 6 and 7

An iterative approach to an accurate bracing design that has the will conclude with the most optimal bracing configuration.

Conclusions, advantages, limitations, and recommendations of the considered wing bracing ideas.

2. Missions Specification and Analysis Methodology

Chapter 2 discusses the background of previously conducted research to determine the most ideal methods of modeling the experiments and justifies the methods that will be used. Benchmarks for this study will also be created, which are determined based on the performance of current airliners. This chapter also outlines the analysis approach that will be used throughout this study incorporating the classical, computational, and experimental methods.

2.1 Mission Design and Specification

The objective of this study analyzes and improves the bracing designs for a long range single aisle airliner and compares its advantages and disadvantages to typical unbraced cantilever wing designs. To monitor the improvements of bracing designs introduced in this study, a currently active airliner will be used as a point of reference. This point of reference is generated based on the previously conducted studies as well as the performance of currently considered successful specifications.

Boeing's longest range airliner is currently the 777 model which has a proven flight path exceeding 8000 miles and available single aisle variants. This design provides a baseline platform to serve as a cantilever comparison and conduct modifications and tests. Previous studies conducted on truss braced wings, including Boeing's SUGAR High designs [3], follow this theory and create a mission profile based Boeing 777-200ER.

Boeing 777-200ER Specifications

Cruise Speed	Mach 0.84 at 35,000 ft
Max Speed	Mach 0.89 at 35,000 ft
Cruise Range	8890 mi

Max Take-Off Weight	297,550 kg
Thrust per Engine	General Electric GE90: 93,700 lb ft (417 kN)

As the focus of this study revolves around the wing and bracing design, the modification and design of unrelated aircraft components is unnecessary. Any changes to the aircraft body add unneeded complexity and additional variables that make the influence of this study's braced wing concept less apparent. For this study, the fuselage and tail will remain completely identical to the control aircraft in structure and geometry. Similarly, the internal structure of the wing will be based on an existing ribbing structure and kept constant throughout each design iteration cycle. The aerodynamic performance of the aircraft is an important factor whenever an aircraft is designed, however due to the structural focus of this paper, a pre aerodynamically optimized design will be picked and maintained throughout these studies. The aerodynamically optimized Boeing 765-095 SUGAR wing will be utilized on a 777-200ER with the following specifications:

	WING Wimpress	V-TAIL Trap	H-TAIL Trap
Area*	1767.20	270.30	314.35
Aspect Ratio*	23.087	1.15	4.48
Taper Ratio	0.173	0.70	0.25
MAC Inches	115.90	185.88	112.46
Dihedral (Deg.)	0.0	-	0.00
1/4 Chord Sweep (Deg.)*	8.02	33.20	30.00
Root Chord (Inches)	194.30	216.44	160.64
Tip Chord (Inches)	33.70	151.50	40.23
Span (W/O Winglet)*	2423.90	211.56	450.68

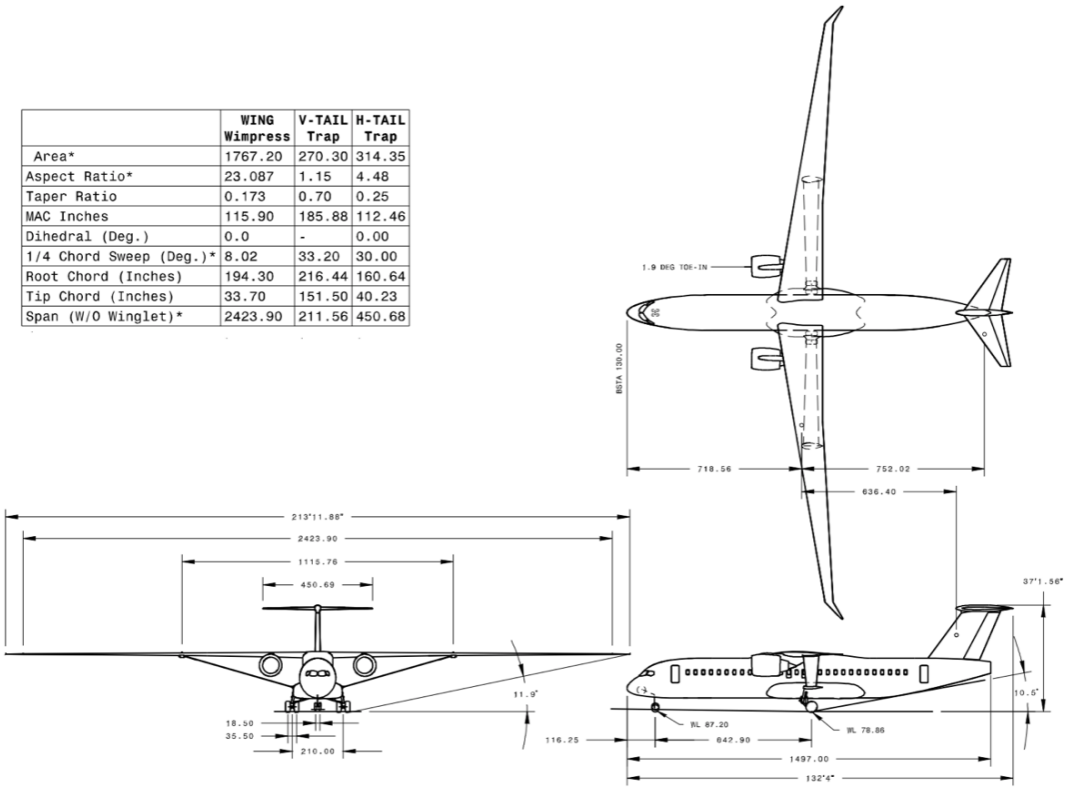

Figure 2 - Boeing 765-085 SUGAR High

The following describes the loading limits and conditions required during this study. They are based on maximum loading factors for transport aircraft and maximum flight speeds of the 777-200ER.

Loading Conditions

Load Factor	2.5G Pull up and -1G Pull Down
Speed	Mach 0.89 @ 35,000ft conditions
Engine Weight	17,400 lb (7,893 kg)
Engine Thrust	93,700 lb ft (417 kN)

2.2 Model of Structure

The definition of a structural model requires the implementation of various forces and mechanical restrictions at various locations of the structure such that the ultimate model simulates all the loads that the structure will endure. These features are called boundary conditions and, in this case, will be selected for the wing to mimic the various loading forces exerted from the aircraft's physical design and aerodynamics forces. Boundary conditions are specific locations on the structure where an interaction occurs whether it be a support of the beam holding it in place or a part or section of the beam with a load applied. These conditions can come in the form of various external loads or internal fixtures limiting displacement and are used to calculate the reaction that the structure exhibits. Changes in the aircrafts net motion will be reflected in the change in the magnitude of these boundary condition values.

2.3 Classical Beam Theory - Analytical

The classical beam theory is the most basic form of analysis to calculate the bending behavior of an elongated structure through the calculation of bending moments, shear flow, and stresses throughout a beam configuration. By observing the magnitude of stress along the wing, a simple demonstration of how the strut affects a wing can be illustrated with conclusions that will be carried on to a more critical analysis. To calculate the mechanical behavior of a wing using this method, the bracing structure will need to be simplified into a simple beam structure. This requires the estimation of the mechanical results of the internal components as these are not directly accounted for in beam theory. Due to the complexity of most structures, this method is not as accurate as modern computational methods. However, classical beam theory is a useful tool for initial proof of concept ideas.

In an aircraft wing application, the main wing and strut will function as their own beam. Unlike a homogenous material, each of these structures in reality are hollow and retain a unique internal structure of stringes, ribbing, and spars that cannot be accurately calculated through

classical beam theory. Thus they will need to be estimated through calculations of the cross sectional area. These types of estimations can indicate a result that might occur from a certain design, however a more accurate model with less assumptions needs to be used for a more conclusive result. To incorporate this, finite element methods will be utilized that can fully model the interior structure in addition to the general bracing configuration.

2.4 Finite Elements Analysis - Numerical

By computationally compiling a mesh of variously sized elements with specified structural properties into a predetermined structure, a Finite Element Analysis (FEA) software can estimate the reaction of complex indeterminate structures. This method of analysis will serve as the primary form of analysis for the completed wing structure that considers all aspects of the structural design that this study analyzes. FEA requires two components to the testing, the modeling component and the analysis component. SolidWorks will be this study's computer aided design (CAD) software, due to its larger computer aided modeling capability, and will be imported into ANSYS structural for continued computer aided engineering (CAE). A parametric method will be utilized to optimize the designs. This will involve the determination of various controlled geometric and material parameters that will be adjusted over each design iteration to form an optimized configuration [12]. As more results are acquired through each design iteration and adjustment, a more ideal structure will be created.

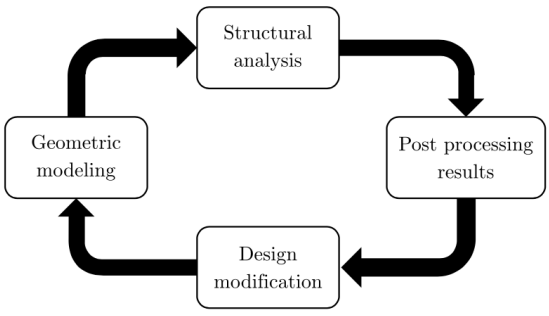

Figure 3 - CAE/FEA design process

Determination of the components to be parametrized will be based on previous conceptual knowledge regarding the structural performance of wing designs as well as the parametric results gained from this study's initial design cycles. This concept is explained in Chapter 3.

3. Existing Bracing Designs

Chapter 2 reviewed and constructed the baseline aircraft setup to be used in this study that related to the non wing bracing related elements. To create an optimized bracing design, initial pre-existing bracing designs that have been successfully utilized in the past will be used as a starting point. This chapter discusses those bracing configurations that will be used as the baselines and previous success and failure with them. The internal ribbing structure of the wing that will be utilized in this study will also be discussed being that the details of the 777-200ER internal wing structure is not publicly available.

3.1 Cantilever Bracing

Cantilever wing designs are the most common wing design used in aircraft due to the relative simplicity of the structure. Due to the absence of external bracing features, the entirety of the wing's structural components are internally mounted. A structural test [13] conducted on an F11 early megaliner cantilever wing [14] deconstructs the wing into several segments of rib, spar, and stringer arrangements.

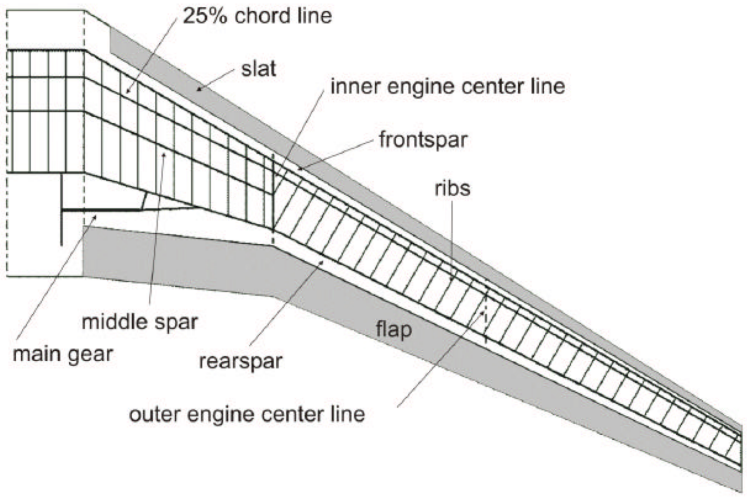

Figure 4 - F11 Megaliner internal bracing structure

The bracing is split into two lateral sections, the inboard section between the root and kink and the outboard section between the kink and tip. The kink is noted as the location where the leading or trailing edge changes it's angle of relative to the span axis. Other than a single net wing spar that runs the entire span, each section has its own set of spars. The inboard section has a significantly reinforced structure with ribs angled with the root and three separate spars. The outboard section incorporates rows of ribs angled perpendicular to the main spar.

The kink is a structural and mechanical housing implementation. The application of the kink provides the area required to retract the landing gear during flight as well as the structural support necessary for the landing gear loads. This is seen on most airliners with landing gears housed within the wing. Another primary factor influencing the bending behavior of the cantilever wing design is the ribbing placement. The ribbing's primary operation is to prevent longitudinal wing flex from leading to trail edge and maintain the airfoil shape under loads.

An aerodynamic consideration in aircraft design is the concept of wing twist. This is the geometric change in the wing's angle of attack across the span of the wing. This adjusts the lift distribution across the wing to yield for more desirable flight characteristics. Airliners have a dynamically designed wing twist achieved through the geometric kink and sweep [11] put into

the cantilever wing. Figure 5 shows the increase in outboard wing deflection when the wing is under load. This is a consideration that will be considered during the addition of bracing as the removal of aerodynamic qualities should be presented during the addition of structural restraints.

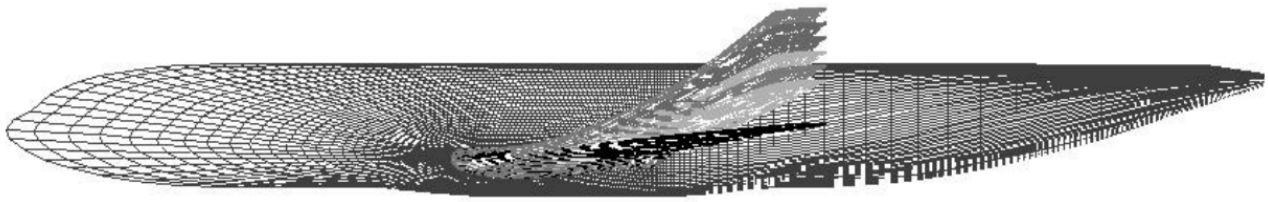

Figure 5 - Deformation of cantilever wing due to rib placement

3.2 Strut Bracing

Strut bracing is the usage of a single external bracing member connecting the fuselage to the wing, usually around midspan. This setup allows the bending stress on the wing to spread through the strut and on to the fuselage. Many strut systems work to brace high wing aircraft by bearing tension while the wing is under vertical loads of lift, however a compression strut can be designed as well to bear loads when the wing is forced in the opposing direction.

Strut bracing, although widely used to control the loads under tension, has problems when compression loads are applied. In a high wing aircraft this would occur with jerk loads during turbulence or taxi bumps. Methods of reducing this effect are through telescoping, arched, or offset struts that allow compressive energy to be absorbed into the other elements of the system while retaining the strut's tensile strength. The addition of hinges at the strut connections are also a configuration that reduces the buckling tendency on the strut [15].

3.3 Strut with Jury Bracing in Aircraft

The truss braced configuration is defined when the wing is braced by not only a strut leading from the wing to the fuselage, but additional members, or jurys, that connect the strut to the wing, see Figure 6. These additional supports provide buckling prevention when the strut is under excessive compressive load. When properly designed, a truss can have the same structural effect as a strut while weighing less.

Figure 6 - Strut and truss braced wing designs tested in SUGAR project

Compared with a solo strut, the addition of a single jury led to the ability to reduce the chord length of the wing as well as the net weight of the wing bracing structure. Multidisciplinary study comparing strut (C100), strut with a jury (C200), and strut with two jurys (C300) during a constrain wingspan and mission profile range, showed that the single strut with a single jury showed a greatest weight improvement and overall performance [6]. By reducing the need for excessive internal bracing and spreading the weight over the jurys, an overall lighter wing design is achieved. Figure 7 shows the weight reduction achieved through the use of the jury implementations over the single strut.

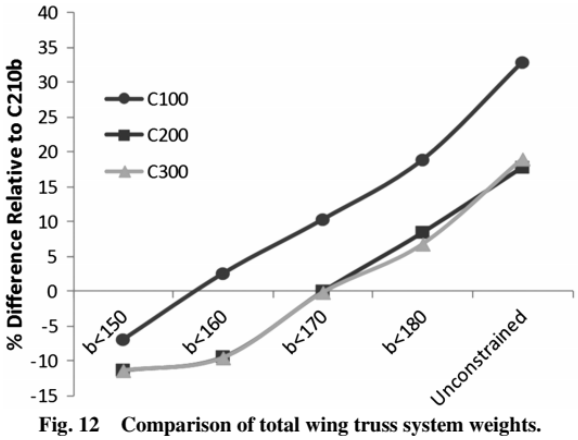

Fig. 12 Comparison of total wing truss system weights.

Figure 7 - Weight Comparison of Strut and Jury Wing Configurations

This particular multidisciplinary study concluded that a strut and single jury layout had the lowest fuel burn during a given mission range regardless of which wingspan was being used. The addition of a second jury showed improvement, but not enough to yield further research.

The three bracing designs with a single strut, a single jury truss, and double jury truss will be incorporated as the baseline configurations during the tests in this paper. An analysis of the influence of elementary design features is required such as strut positioning and placement to observe the reactions that a wing would have to wing bracing mechanisms and prepare for a more in depth optimization through FEA.

4. Bracing Analysis Through Classical Beam Calculation Methods

Before a full fidelity simulation including more complex variables and consideration is utilized, a simple model of a beam supported by a strut at various locations is created to simulate the behavior of a wing under loading during cruise. Although rudimental, it is accurate enough to gain an understanding of how a strut system would react under flight conditions. This chapter reviews the geometry setup, loading constraints, and stress results of struts positioned at various positions along the wing span. In addition to the classical beam simulation of the braced wing, the model used for the elliptical lifting load is also explained.

4.1 Application of Simple Beam Theory in Strut Bracing

Simple beam calculations are computed to demonstrate the fundamental effect of bracing supports on a cantilever geometry. This is to give an outlook on the effect that the various bracing mechanics will have on a simple beam structure. The goal of this structure is to reduce the bending stress across the span so that the maximum stress in the structure does not approach the maximum bending stress of the materials being utilized. The calculations will show the bending stress across the span or the wing and allow for further improvement on the brace based on the bending characteristics that each configuration displays.

The initial calculations are conducted on a simple cantilever configuration to display the preliminary vertical stresses that typical aircraft operating conditions such as weight and lift exert on the wing. A second, third, and fourth configurations utilize a strut brace connected at varying positions along the wing span. The addition of a strut will result in a reduction in maximum bending stress, however a test of the spanwise position sweep will show the benefits of the various spanwise positioning.

4.2 Applied Loading and Simplification of Wing Model

The configurations will be calculated based on the following model displayed in figure 8 Fixed supports are positioned at the wing root and strut root of the wing. An elliptical lifting load is distributed across the wing span. A uniformly distributed load is exerted across the length of span of the wing that is equal to the half span wing weight of the Boeing 777-200ER. A vertical point load is placed 12m from the root of the wing with a weight equal to that of the GE90 Engine used on the Boeing 777-200ER. Tension of the strut is also incorporated as a point load at various points during each calculation and the magnitude of the vertical contribution is calculated based on the methods described in 4.2.2.

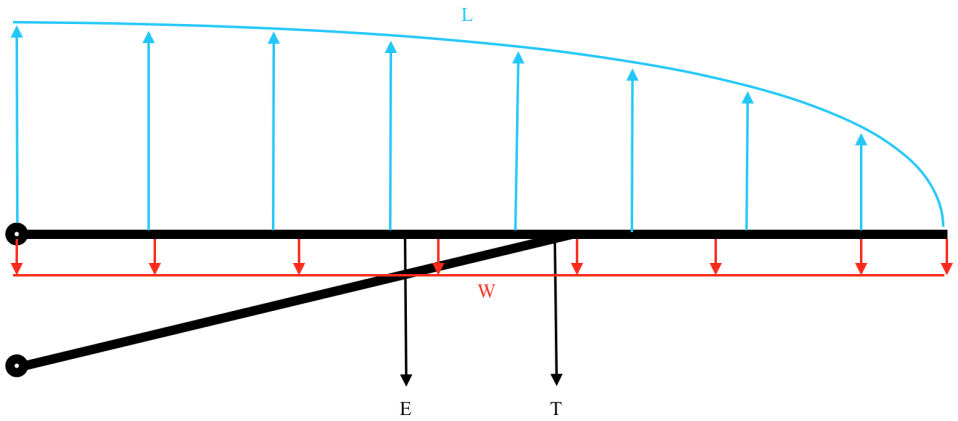

Figure 8 - Free body diagram of vertical loading on beam simplification

4.2.1 Lifting Load

The lifting load on the wing is derived from the Lanchester-Prandtl wing theory that assumes an elliptical lift distribution due to the vortex strength of the lifting line losing strength as it nears the wing tip[16]. This is mathematically derived based on the net lift that the wing is generating as well as the geometry of the wing itself.

The elementary model of a finite wing is modeled by a horseshoe vortex that, due to characteristics of the airfoil such as camber and angle of attack, runs the length of the wing. However this model is overly simplified and incorrectly runs uniform throughout the wingspan, immediately dropping to zero as it sheds at the tips of the wing [16]. A more realistic elliptical model is formed through the summation of additional horseshoe vortices that shed at various points within the wingspan at the trailing edge in a net vortex sheet. This summation of vortex lines and circulation magnitudes Γ shown in figure 9.

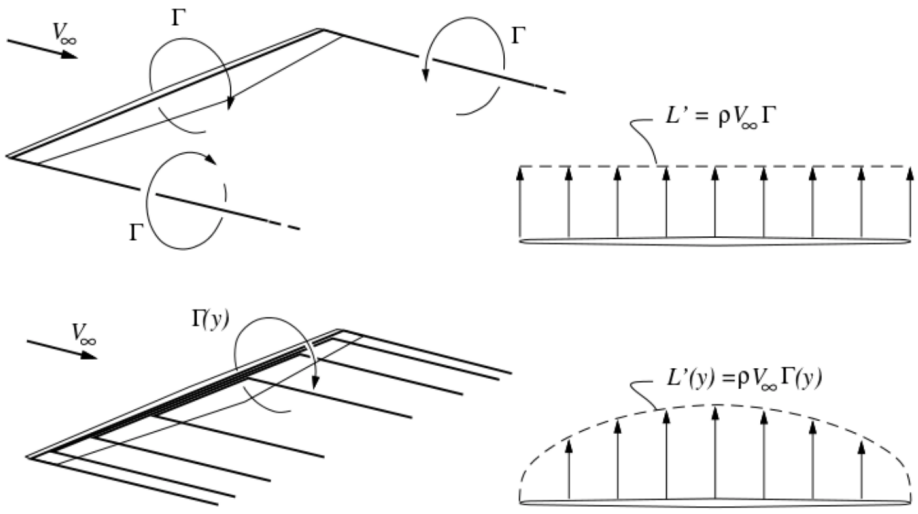

Figure 9 - Single horseshoe vortex and summation of vortex sheets

Beginning with the Kutta- Joukowski equation that relates lifting force to circulation

$$L'(y) = \rho V_{\infty} \Gamma(y) \tag{1}$$

the is spanwise lifting load is expressed as

$$L(y) = \frac{4L}{b\pi}\sqrt{\left(1 - \left(\frac{2y}{b}\right)^2\right)} \tag{2}$$

which models the lifting load at each point y per unit span across the wing of length $b$with a net lifting force L.

The maximum takeoff weight of the Boeing 777-200ER is $297550\ kg$. Assuming an equilibrium condition, the total lift necessary to keep the aircraft at cruising state is equal to the weight of the aircraft itself and the net lift used in the lifting line plot reflects this. A MatLAB script incorporating the lift distribution for the half span of the 30.5m wing through the Prandtl lifting line theory is shown in figure 10. This distributed load is used for the lift contribution in the future beam theory calculations.

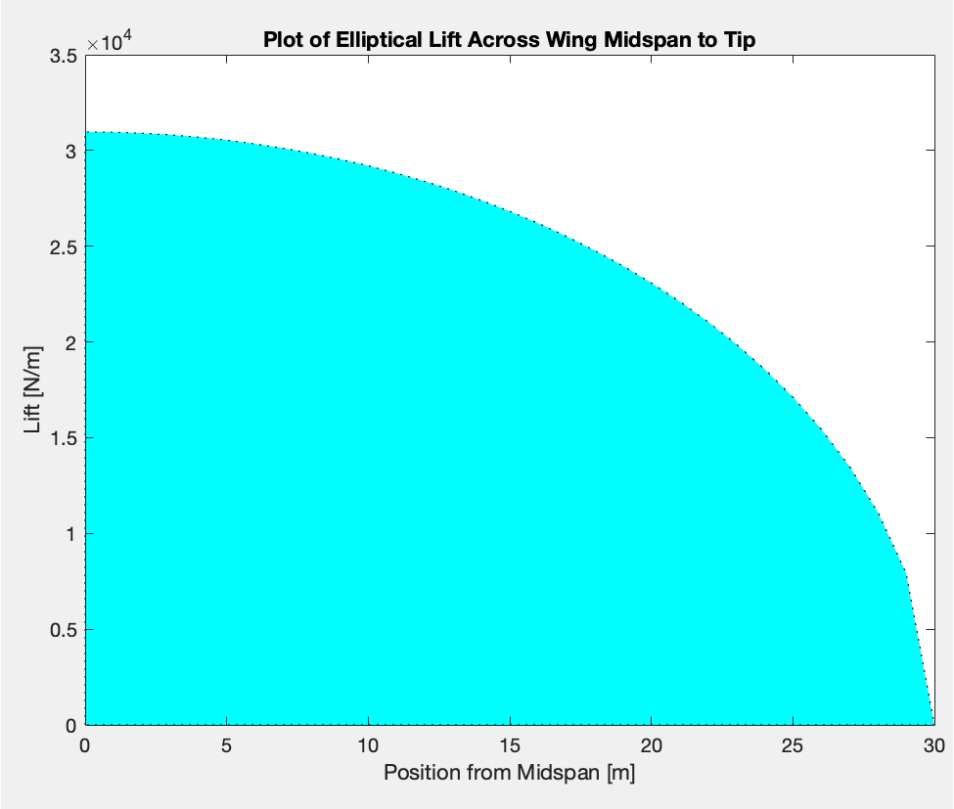

Figure 10 - Plot of elliptical loading over a half span of Boeing 777-200ER wing

4.2.2 Wing Equilibrium

The vertical component of tension applied at the struts connection on the wing is calculated through the condition that the wing is under static equilibrium. With the net moment

applied equal to zero, the tension applied by the bracing is determined through the summation of all the moments in the system about the root, equation 3.

$$\Sigma M_{root} = 0 = -Ed_E + Ld_L - Wd_W - Tsin\theta d_T \quad (3)$$

The distributed loads of both the wing weight and lift are condensed into point loads for implementation into the moment equation. As the distributed load of the wing weight is uniform throughout the span, it is applied as a point load at the center of the wing's half span in the moment diagram. The elliptical load of lift is not uniform and therefore cannot be reduced to a point at midspan like the wing weight and requires a separate method, equation 4, to find the horizontal centroid $\overline{y}$ from the midspan point. Figure 11 shows the diagram of the resultant loads acting on the system.

$$\overline{y} = \frac{\int_i^f yL(y)dy}{\int_i^f L(y)dy} \quad (4)$$

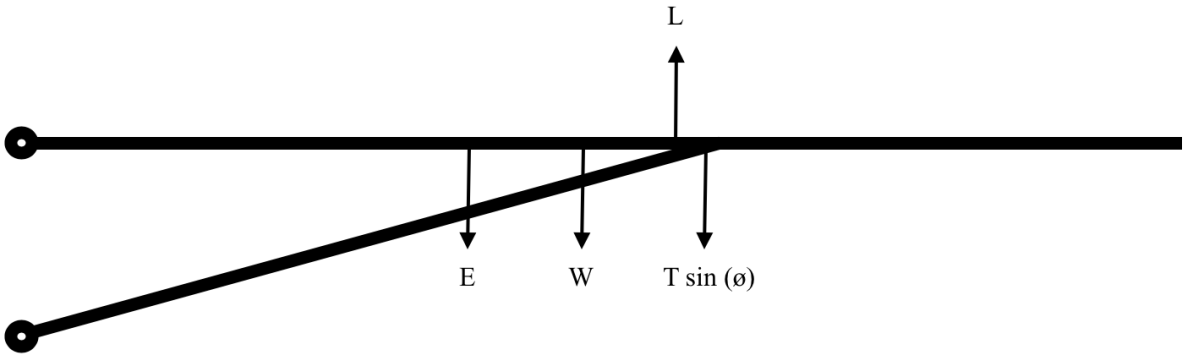

Figure 11 - Reduced loads on wing

4.3 Generation of Stress Plots

To determine the stress in the wing, the geometry of the cross section is defined as a solid rectangle of height 1m and length 10.3m, the root chord of the Boeing SUGAR 765 -085. Stress, calculated by equation 5, is a function of the moment at that section, the moment of inertia and position on the cross section.

$$\sigma = \frac{My}{I} \tag{5}$$

The stress diagrams are derived from bending and shear diagrams. These are determined by cutting the wing into a finite number of sections for which the moments and net vertical loads are calculated for [17]. As each section's moments build upon each other moving toward the root of the wing, each section's moment is equal to the summation of all the moments in the sections farther outboard. Figure 12 and 13 illustrate the concept used for calculation of the bending moment and shear force distribution across the beam. The beam is split into multiple sections in which the loads are averaged at their center. Figure 12 shows one of those sections with its individual moments and shear forces.

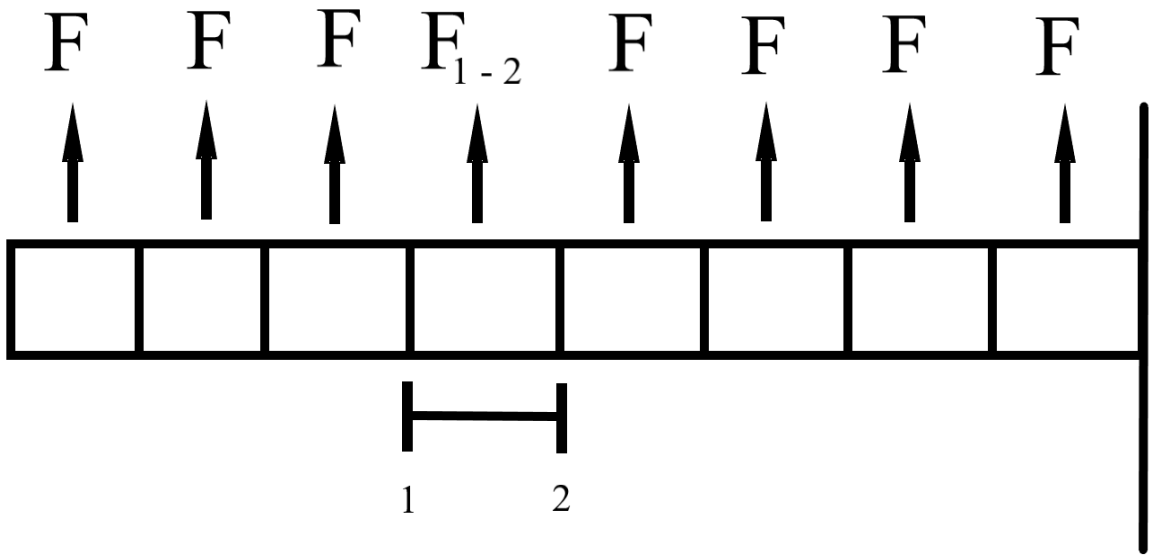

Figure 12 - Beam cut into sections for distributed load calculations

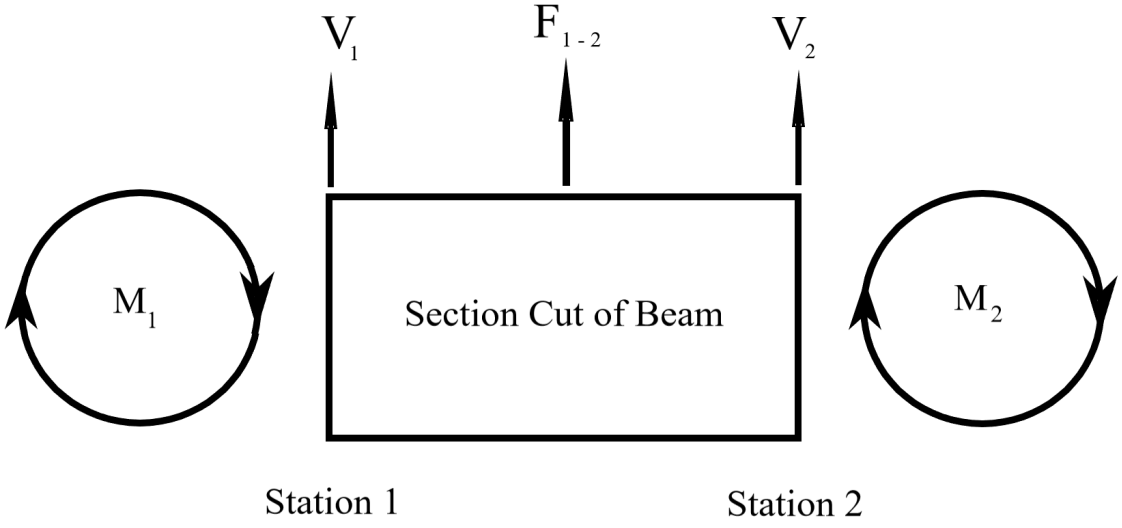

Figure 13 - Section cut of the beam with free body loads

V_1 Shear at the left side of the section, station 1, is equal to the summation of all the shear forces of the sections to the left of that section. Similarly the shear to the right of the section, V_2

is equal to the summation of the shear V_1 and the F_{1-2} force applied at the center of the section. That shear is used for the following section to the right and so on until all the shears at each station are known and can form an observable plot.

$$V_2 = V_1 + F_{1-2} \tag{6}$$

Moments are calculated in a segmented manner as well. The M_1 moment to the right of the section, station 1, is calculated through the summation of all the moments of the forces to the right of this section about station 1. The moment about station 2 is the summation of the moment at station 1, moment caused by the force load about station 2, and moment caused by the shear at station 1 shown in equation 7.

$$M_2 = M_1 + \frac{1}{2}F_{1-2}d + V_1 d \tag{7}$$

The compilation of these calculations is numerically compiled into an excel sheet that calculates the loads at each station to form the plots of bending moment and shear.

4.4 Results and Discussion

The plots of each configuration show the effect that the addition of a strut and widening of the struts connection position have on the 30.5 meter wing. The shear plot depicts the largest shear load exerted on the beam at the root, coinciding with the theory stated in section 4.3 that shear and moments are summed across the span of the wing leaving the root bearing the load of the entire wing and the tip bearing no load of the wing. In addition, there is a clear increase in shear force at 12 meters where the engine loads the wing. Due to the resolution of this plot being 0.5 meters, the shear increase is sloped, however a point load like this would result in a stepped result at 12 meters. The same concept applies at the points of strut connection at 13 meters, 20 meters, and 30 meters for each pertaining plot although the effect is amplified.

As the bending and stress functions are proportional and differentiated by only the constant moment of inertia and position on the cross section, they portray the same result with differing magnitudes. In this case, the stress is taken from the highest point on top of the wing. Similar to the shear force, the bending moment is maximum for the cantilever configuration at the root due to the summation of all the moments building up at that location and decreases to zero at the wingtip. The addition of a strut reduces this peak moment by spreading it through the strut itself.

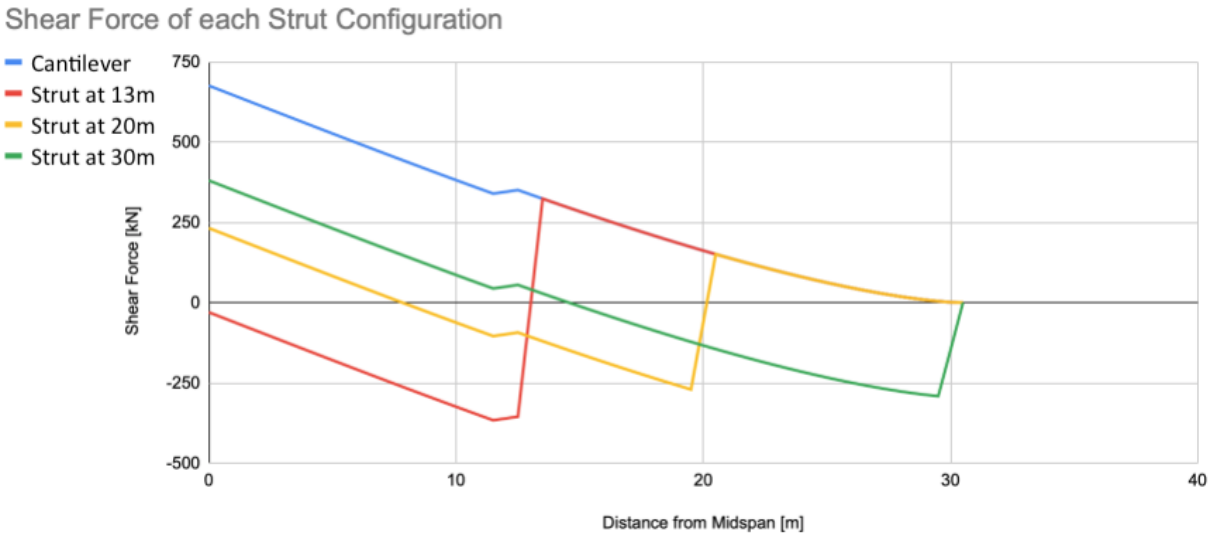

Figure 14 - Shear force results from strut position sweep

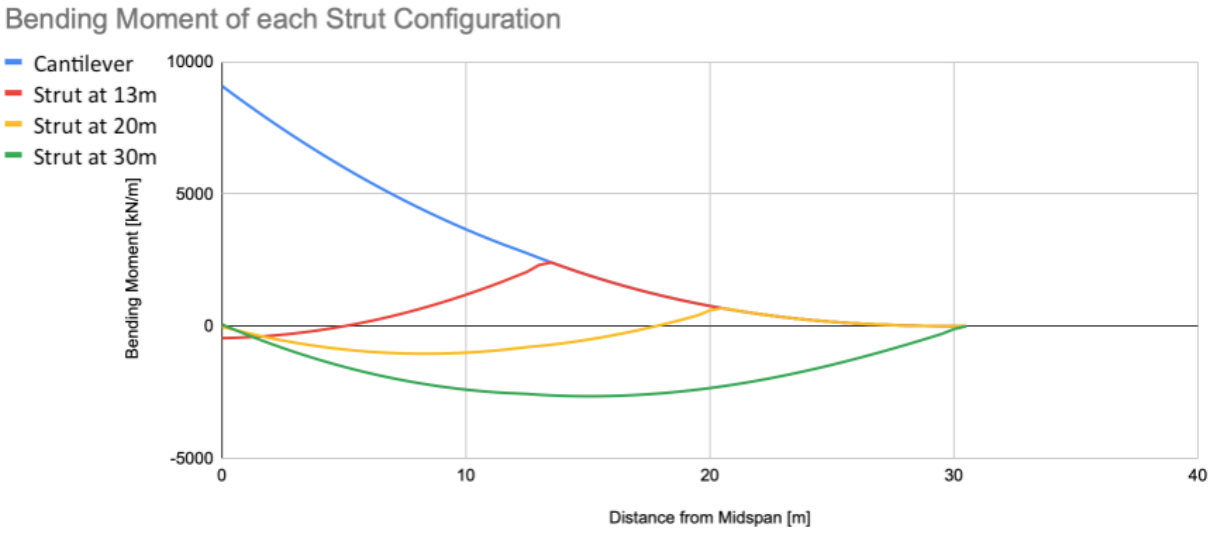

Figure 15 - Bending moment results from strut position sweep

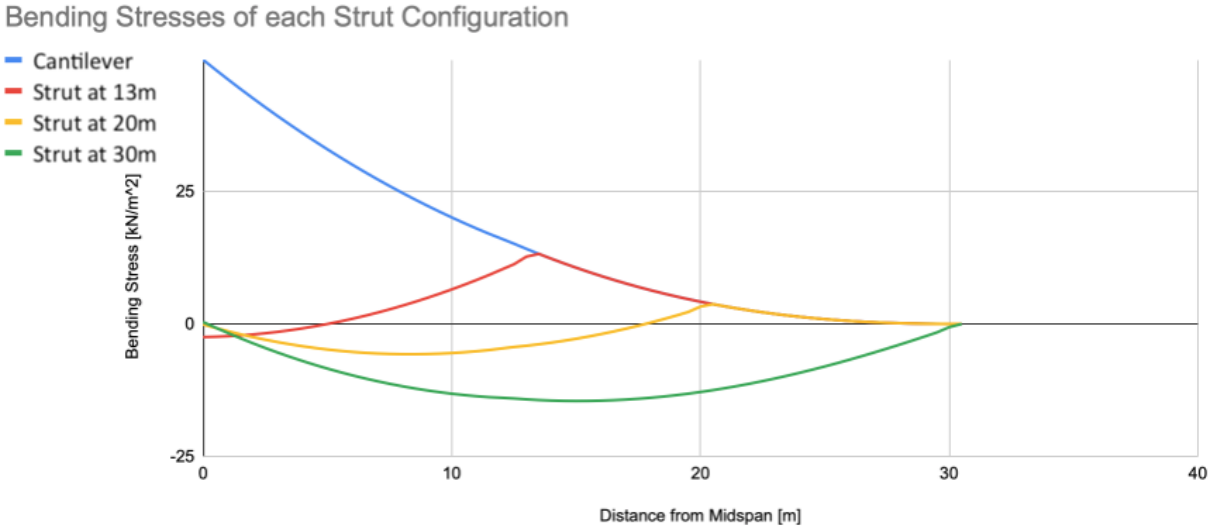

Figure 16 - Bending stress results from strut position sweep

The plots of each configuration indicate the advantages and disadvantages of adding a strut. The introduction of a strut in all cases results in a reduction in the maximum bending stress. Although a strut addition regardless of location reduces stress on the wing root, the wider the strut is placed on the wing, the larger the negative stress on the wing. The addition of a strut lowers the dependence of the wing on its internal bracing due to the lower stresses seen allowing

for less weight bearing materials, however the peaks of bending moment located at the point of the strut exhibit a plausible problem for the strut component. Being that struts and trusses are designed for extension and compression, any strut undergoing this any type of twisting load like a moment is unideal. A possible consideration in further designs should be the implementation of a hinge that would allow the strut to perform without the introduction of moment.

Although rudimental, the figure 15 shows that the addition of the struts does reduce the stress along the span of the wing. This allows for a reduction in the required material used within the internal wing structure itself, which would be beneficial in the weight high aspect wing design. However the simplified model leaves out variables such as wing twist, thrust, longitudinal, strut placement, and internal structure contributions that will be accounted for in future chapters. Based on the results, a strut design with a strut placed at between the 13 and 20 meter position yields the lowest peak stress. These designs however place unsuitable stress loads on the strut insertion point itself which will have to be considered when running more in depth simulations.

5. Baseline Structural FEM Analysis

In the previous chapter, the bending behavior of the wing structure was approximated through a “quick and dirty” classical analysis. This section begins the iterative FEA design process with the baseline wing model without any external bracing. This chapter establishes the baseline wing geometry and boundary conditions, to allow for a controlled adjustment and observation of input and output geometrical variables throughout future design iterations. This baseline wing structure is then evaluated and modified for later design iterations of the externally reinforced wing models.

5.1 Finite Element Method Overview

FEA is used to analyze the baseline aircraft truss structure and make iterative adjustments to optimize the truss geometry. As a base airframe structure, the F11 megaliner frame, shown in figure 4, is used and adjustments are validated through the FEA process. The FEA process begins with the modeled CAD shape and is exported into ANSYS. With the proper loads and joints accounted into the system, a modal analysis is run to visually validate that the wing structure is bending as it is supposed to and that the joints are bending and moving within the constraints of geometry. Once complete the loads are used for a full static load simulation so plot the characteristics of the structure in terms of stress, strain, and displacement. Results of the simulation are reviewed for a design change and rerun in a new iteration.

5.2 Baseline Wing Ribbing FEA

This section begins the FEA design process by constructing the baseline wing platform for which modifications in future design iterations will be made. This first iteration of the wing defines the initial behavior and characteristics of a wing without any external bracing. As the goal of this study is to decide what parameters are to be optimized for this unique high aspect

ratio geometry, the 30m half span SUGAR wing geometry is used for all of these studies. There are no developments on the specific internal bracing structures associated with the SUGAR wing, thus the internal structure for this wing will use a similar setup to the F11 Megaliner wing.

This configuration incorporates all the mandatory boundary conditions, geometry specifications, and mesh sizes used for the future design iterations defined in the following section 5.2.1. Being that the loading parameters stated in chapter 4.4 classical formulation method are the same, a comparison will be made between the FEA model and the classical calculations to validate results and show how the differences in geometry are affecting the stress curves. These differences will be a result of more detailed models that include ribbing, spars, material, sweep, and external wing shape. Specific areas of high stress and strain will be observed and adjusted for during later design iterations when the external bracing are added.

5.2.1 Baseline Wing Geometry Configuration and Modal Check

A high wing, high aspect ratio internal wing structure geometries such as the SUGAR wing are not publicly released, however the external dimensions are public. This being, the external geometry of the high aspect ratio SUGAR wing is used in this study with an internal structure based on a different wing model. The previously discussed F11 Megaliner wing, shown in figure 17, being another internal airliner geometry setup, will be used as a reference to construct the internal frame structure of the SUGAR wing for this design process. This frame like the F11 structure runs a set of longitudinal main ribs running parallel to the direction of flight and a set of ribs running perpendicular to the secondary aft spar. As the SUGAR wing has a thinner chord, the two center spars seen on the F11 wing are not transferred over. The main front spar has a 0.2m thickness while the secondary aft spar has a thickness of 0.1m. The reasoning behind this is that the aerodynamic loading will be loaded at ¼ chord, where the main spar is, thus the main spar will be taking the majority of the load while the secondary spar will primarily be resisting wing twist. Both spars also have different sweeps throughout the length of the wing. The main spar follows the same 15 degree sweep as the leading edge of the wing,

while the secondary spar follows the sweep of 0 degrees from root to kink, and then shifts sweep to follow ¾ chord. The ribs are all set to a thickness of 0.015m.

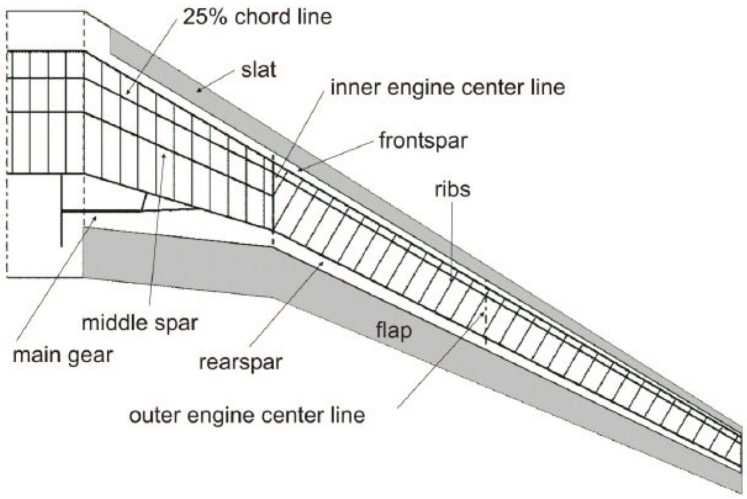

Figure 17 - F11 Megaliner wing frame layout

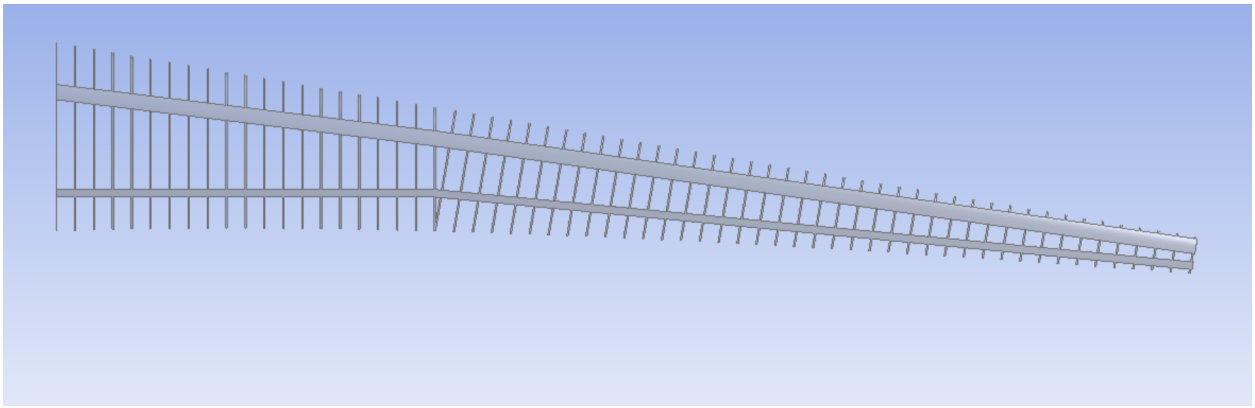

Figure 18 - SUGAR Wing internal frame structure based on F11 Megaliner frame

A concept used throughout all these design iterations whenever a new connection or boundary condition is added, is a modal check. This checks for breakages in the geometry and ensures that the model is reacting in an expected manner under each mode. The simulated results show the bending shapes as a result of the various modes and reveal any improperly connected interfaces that are not visually reacting as they should. A simulation that fails a modal check could result in a failure to solve when inputted in a full static structural simulation. Figures 19-22

show the total displacement results for frequency modes 1, 2, 3, and 4 of each of the modes for the properly constructed cantilever wing that is used for a static simulation without any geometrical breakages.

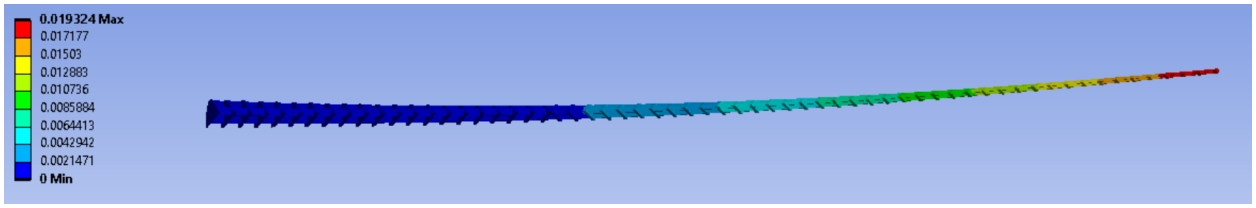

Figure 19 - Mode 1 total deflection modal analysis

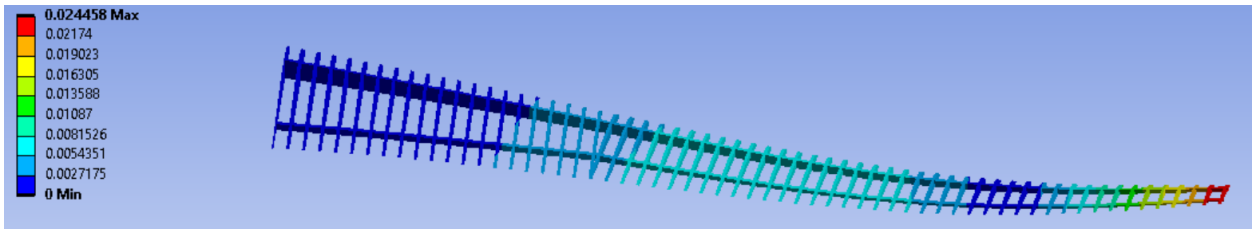

Figure 20 - Mode 2 total deflection modal analysis

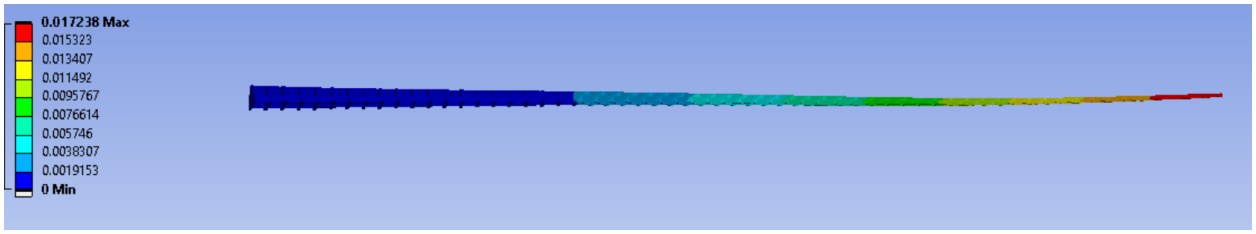

Figure 21 - Mode 3 total deflection modal analysis

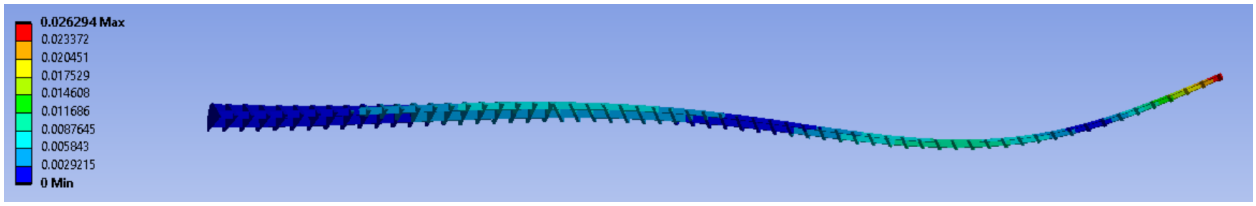

Figure 22 - Mode 4 Total deflection modal analysis

5.2.2 Mesh Optimization

Although a constant sized mesh can accurately model the shape of the aircraft wing for a simple modal analysis, a more detailed meshing scheme is used for the actual simulation model

to run static structural analysis. A mesh sizing of 0.075m with tetrahedrons is used as a mesh. Figure 23 shows results of this mesh with no deformed surfaces and edges.

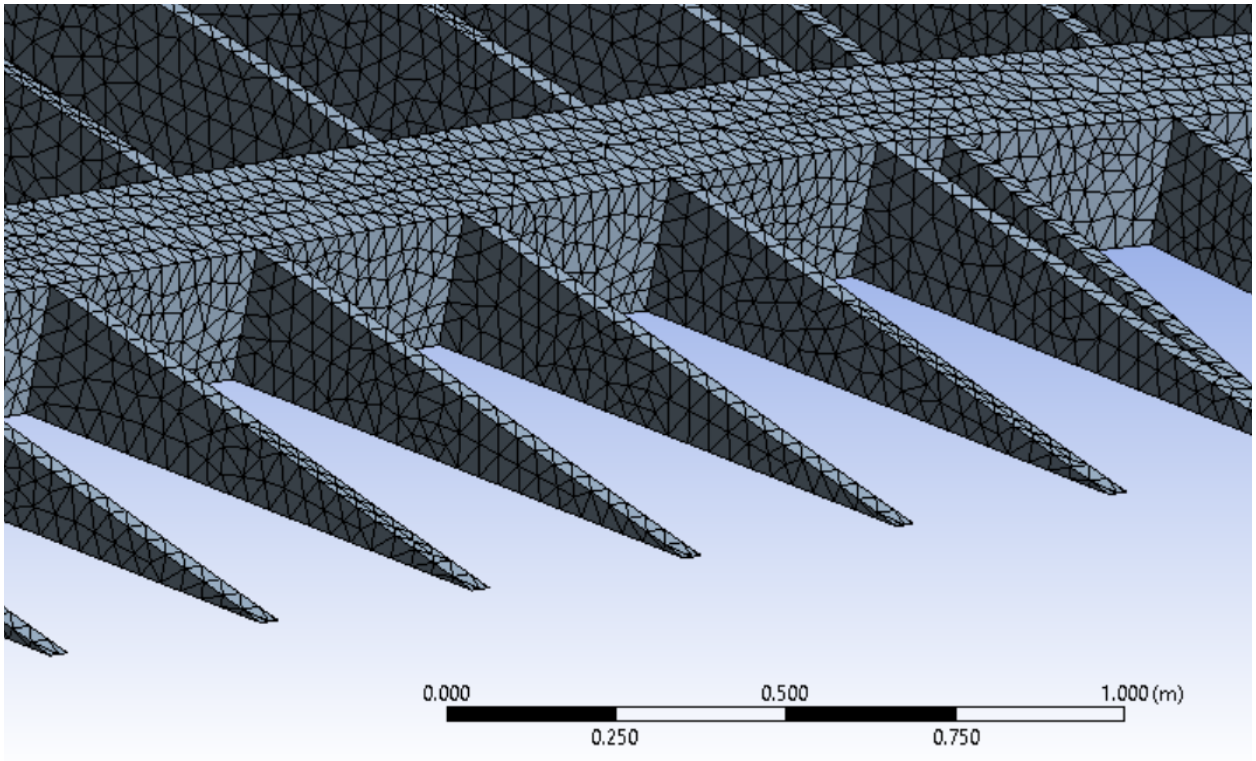

Figure 23 - Main wing mesh at 0.05m tetrahedron

5.2.3 Base External Loads and Boundary conditions

There are multiple boundary conditions and constant loads that are exerted on this model that are covered in this subsection. To support the wing, this model runs a static loading condition with a fixed wing root. As stated in chapter 2, the weight and material specifications used for the baseline study are retrieved from Boeing's current longest range airliner, the 777-200ER, that the NASA SUGAR aircraft is compared to. The wingspan is baselined at 61.5 meters and the weight of the aircraft is set to 297,550 kg which is 2918965N with gravity and 1,459,482N for the half span study. A load of 2.5G is placed on the wing for the maximum designed loading on the airliners discussed in Chapter 1, a safety factor is added in the results of the model to ensure the wing will be able to handle some caliber of irregular conditions as well. The weight of each GE90 engine placed 4.5m from the root is 7,893 kg or 77430N with earth gravity. Material choice is set to aluminum alloy with a Young's modulus of 71 GPa and yield

tensile strength of 280 MPa. This material property is also used to calculate and exert the standard gravity loads from the weight of the wing itself, applied throughout the geometry of the wing.

Aerodynamic loading is applied to the half or full span of the wing through the elliptical loading described in Figure 10 of Chapter 4. The equation is written as

$$L(y) = \frac{4L}{b\pi}\sqrt{1 - \left(\frac{2y}{b}\right)^2} = \frac{(4)(297550)(9.81)(2.5)}{(61.5)(\pi)}\sqrt{1 - \left(\frac{2y}{61.5}\right)^2} \quad (8)$$

which leads to the half wing loading chart as follows.

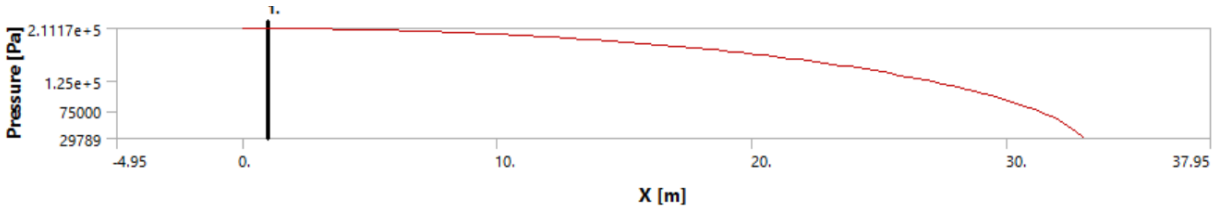

Figure 24 - Elliptical Loading result for baseline pressure loading across half span length

This aerodynamic loading is applied to the wing at the ¼ chord spar to simulate the load at the longitudinal aerodynamic center of the wing. Although these constraints are run for the internally braced wing, additional constraints including a revolving pin, and ball joint are used in later design iterations.

5.3 Baseline Cantilever Wing Results

Observing the results for the baseline cantilever wing, there are both similarities and differences that are seen from this comparison. A solid wing without spars is initially run to display the behavior that the external wing geometry itself without internal complexities elicits. Unlike the classical calculations conducted in the previous chapter, the geometry of the wing does not display uniform bending deflection as the chord length is not consistent throughout the

span of the wing. There is a wider chord at cross sections closer to the wing root and the wing tapers at different rates at the sections in and outboard of the kink. These geometric differences result in the wing's internal stresses being different at varying positions along its span. This variation is shown in the span wise stress plots.

In figure 26, the stress across the bottom surface of the main spar as a function of the distance from the root is shown. There is a definite difference in the behavior of the wing specifically from the root to ~10m. In this section the classical calculations show a decreasing stress, however the FEA model shows an increase in stress that tapers as it reaches ~10m.

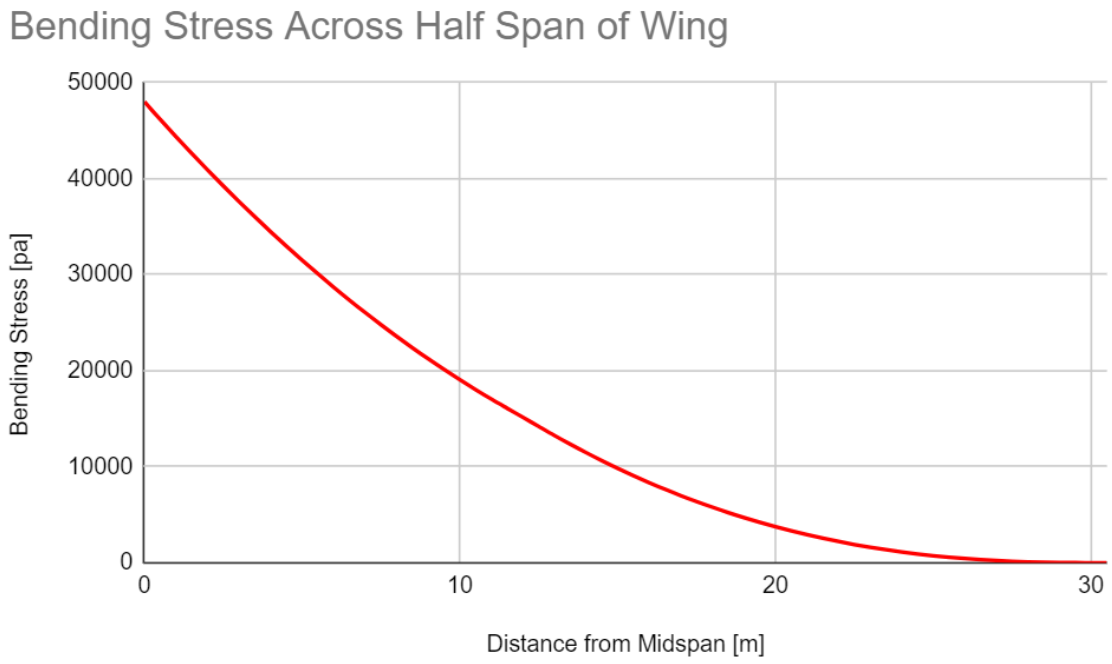

Figure 25 - Bending stress of classical calculation

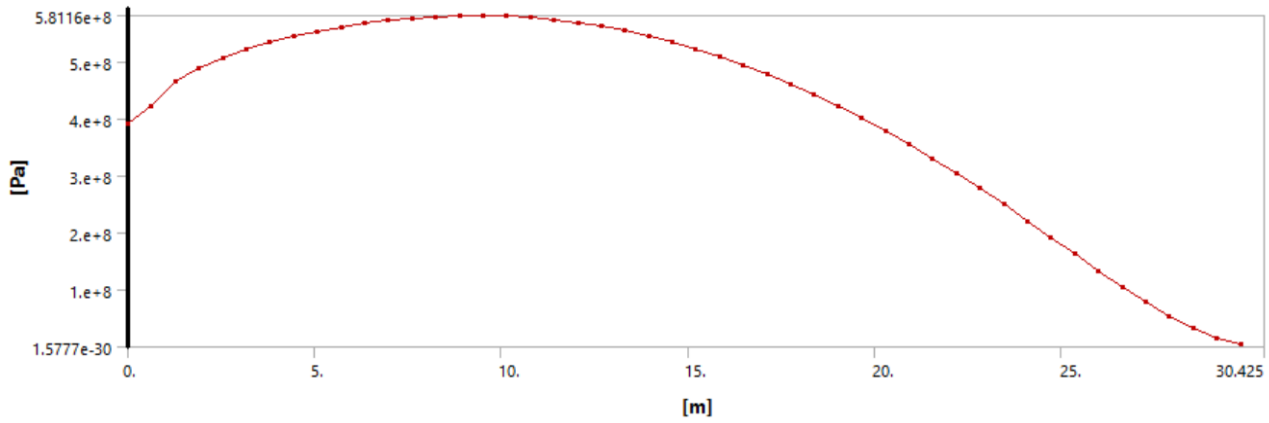

Figure 26 - Solid SUGAR wing main wing stress across span of wing

This behavior is something more inline with what is seen in a beam supported on both sides as there is a decrease in bending stress not only at the tip of the wing, but at the root as well. Figure 27 shows how the peak in stress is seen across the middle of the wing. As the loading and boundary conditions are the same between the two plots, it is concluded that the peak in stress is due to the external shape of the SUGAR wing.

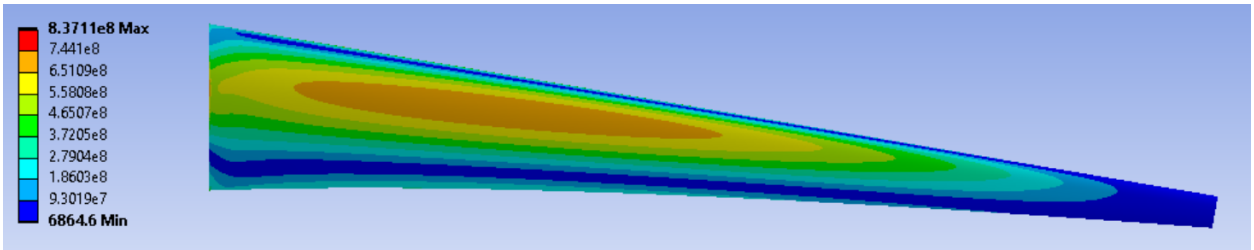

Figure 27 - Maximum principle stress shows behavior of tapered wing [pascals]

In this study, the feasibility of the wing to perform is based on whether or not the wing takes permanent damage under the maximum loading conditions and safety parameters defined in the previous section. The wing will permanently bend if the stress at anypoint exceeds the maximum yield stress, thus stress is used as one of determining factors as to whether the wing is a structurally adequate design. A factor of safety of 1.5 is used when considering the design requirements for a civil aircraft [18]. In addition to the max 2.5 G load defined by the SUGAR

aircraft flight parameters. Figure 3 shows the stress distribution in the form of a factor of safety on the frame of the wing.

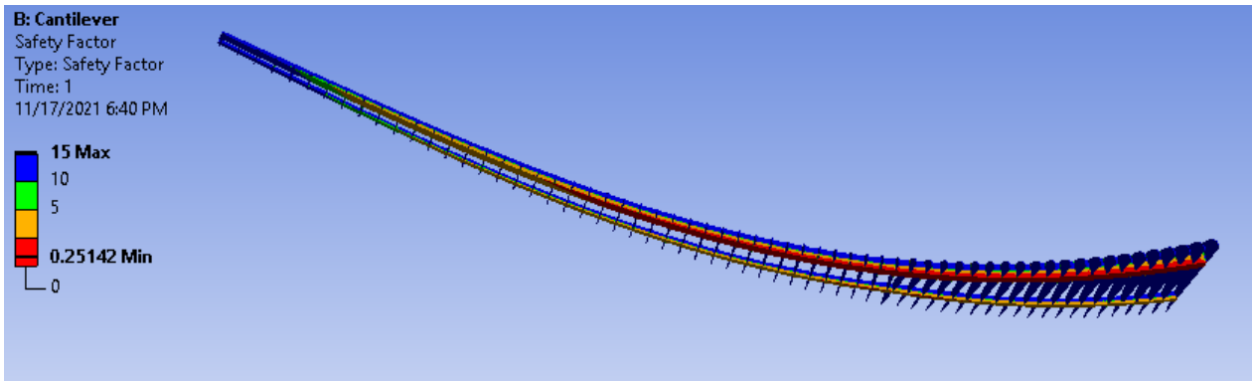

Figure 28 - Based on this study of stress, the wing has a minimum 0.251 FOS and would yield to failure

The stress on the wing is out of range of the yield stress of the material and fails at a factor of safety of 0.25. The majority of stress is seen on the main spar with the maximum stress being seen between the kink and root, however the stress is below the range of the 1.5 FOS limit throughout ~75% of the spar. This frame layout exceeds the maximum yield stress of the aluminium material and will permanently bend under the aircrafts load. Because the wing has such a low FOS, a solid wing design will be run to ensure that a frame can be designed to support the wing structure. A solid wing is the best case scenario for this exterior wing geometry as that ensures that there is the most material incorporated as possible to resist bending. As the stress of interest in this case is seen below the wing, it is a result of the lifting force. The extra weight of the material will only benefit the scenario by loading the wing in the opposing direction to lift. Figure 29 shows the stress distribution as a factor of safety on the solid wing.

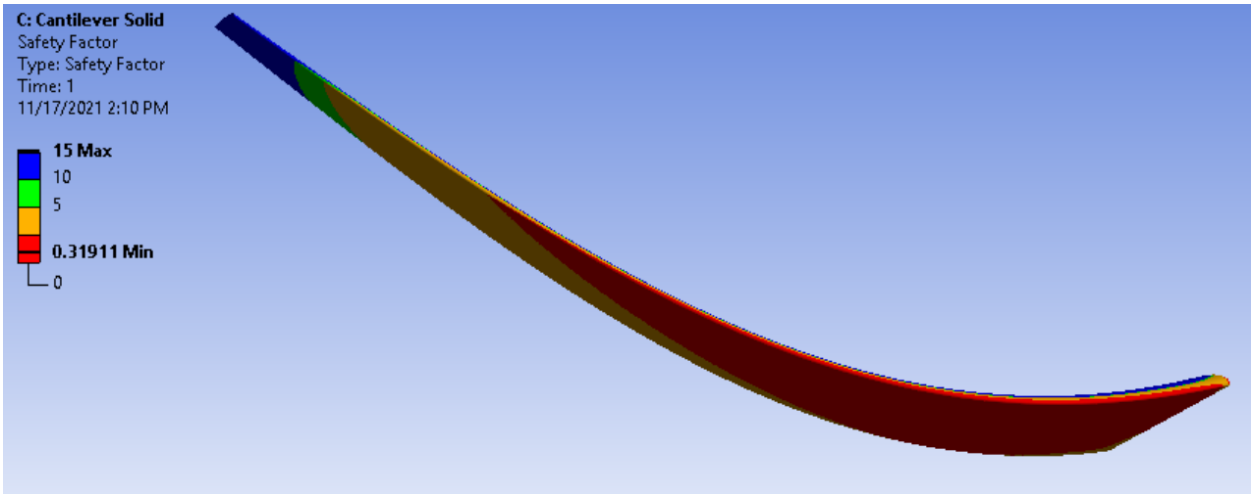

Figure 29 - 0.32 Factor of safety of stress on solid cantilever wing shows a failed result

The aluminum material under the provided same lifting load will fail at a FOS of 0.32 with a completely solid wing. The stress along the wing does improve with the increase in material, however the FOS is far below the required 1.5 value. This concludes the design iterations for the cantilever setup. Without changing the material or external geometry, there is no way to internally brace this cantilever design under the defined loads. This solid wing represents an unachievable, yet physical best case scenario and cannot perform without surpassing yield stress of the material.

6. Design Iterations for Strut Setup

Chapter 5 began the iterative design process by analyzing the baseline wing geometry and determining the best design for a cantilever setup. Without changing the exterior shape of the wing, this design was found to fail in every case and thus could not be optimized further. This chapter begins design iterations with external bracing designs utilizing a single reinforcement strut setup. The initial design is created with a strut and rerun with improvements during each iteration to determine the factors that affect the struts performance and create an overall design that will support the wing under the SUGAR defined loads.

6.1 Strut Bracing Overview

The strut configurations run in this study are considered to be a single solid beam running from an anchor point on the fuselage to another anchor position along the span of the wing to counteract the twisting moment caused by the lifting force of the wing. Many aircraft incorporate a hollow strut to keep the weight down while retaining geometrical flexibility to manipulate the aerodynamic cross sectional shape of the strut. The idea of using a completely hollow strut is initially considered, however an alternative method is determined to be a more effective use of both processing and design power. An organically shaped hollow tube design requires more geometrical considerations especially with incorporation of more complex pin and slider joints. This being, a solid rod is initially used for the iterative design process until a successful design is conceived with quantifiable performance requirements for the strut itself. Once the entire wing assembly has been designed with a solid rod, a hollow rod can be incorporated by designing the strut part as an individual component. Knowing the loading conditions on the solid rod a hollow strut can be designed to perform under the same conditions. This allows for the design of the solid strut member first, before considering the complex hollow assembly.

6.1.1 Strut Design Iteration 1

The initial setup utilizes the same frame wing geometry described in figure 3 of chapter 5. The wing is braced with a single rod anchored 5 meters below the base of the wing to simulate an anchoring position at the base of the SUGAR aircraft fuselage that is ~5 meters in height. The other end of the strut is fixed to the wing on the main spar at a position 20 meters in the horizontal direction away from the root of the wing. The aluminum rod is 0.3 meters in diameter. The strut is positioned exactly perpendicular from the freestream.

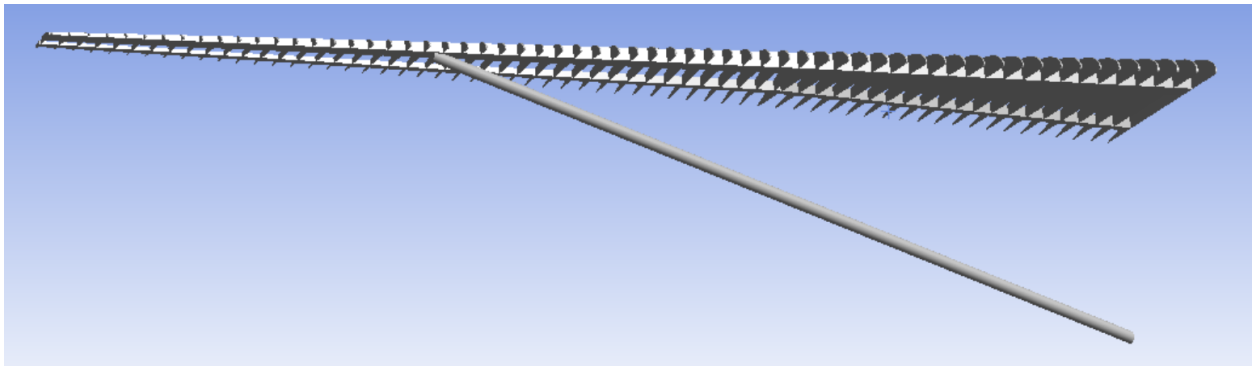

Figure 30 - Geometry of Strut Braced Wing

Observing the results from all the vertical wing loads, the comparison between the undeformed and deformed model shows that the wing not only displaces in the vertical direction, but in the horizontal direction as well. Figure 31 illustrates how the strut during its peak load is located 0.48 meters behind its initial unloaded position. The ideal loading conditions for the strut, acting as a truss member with the wing, should not incorporate this type of translational movement. The translation is a result of the strut not being positioned in line with the main load direction of the wing. Being that the strut is stiffer under extension then deflection, when the wing sweep and strut are not angled parallel in the same direction, the strut accommodates the deflection by deflecting about its root joint and thus limiting the amount it extends. This also results in undesirable lateral wing displacement in the horizontal direction shown in figure 34. High stress is seen on the sides of each of the ribs. The high stress on the top of left and bottom right of every rib relative to the image show that the ribs are shearing due to the secondary spar moving in the opposite direction to the main spar. With the improved positioning of the strut described

previously, a decrease in the stress should be seen on these ribs as the wing's translational displacement is reduced.

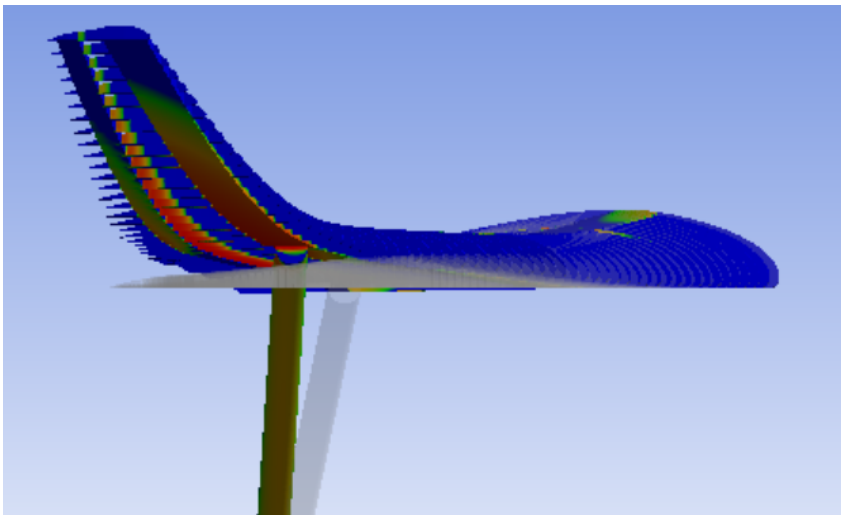

Figure 31 - Deflection in strut and translation in wing due to angle of strut with respect to wing

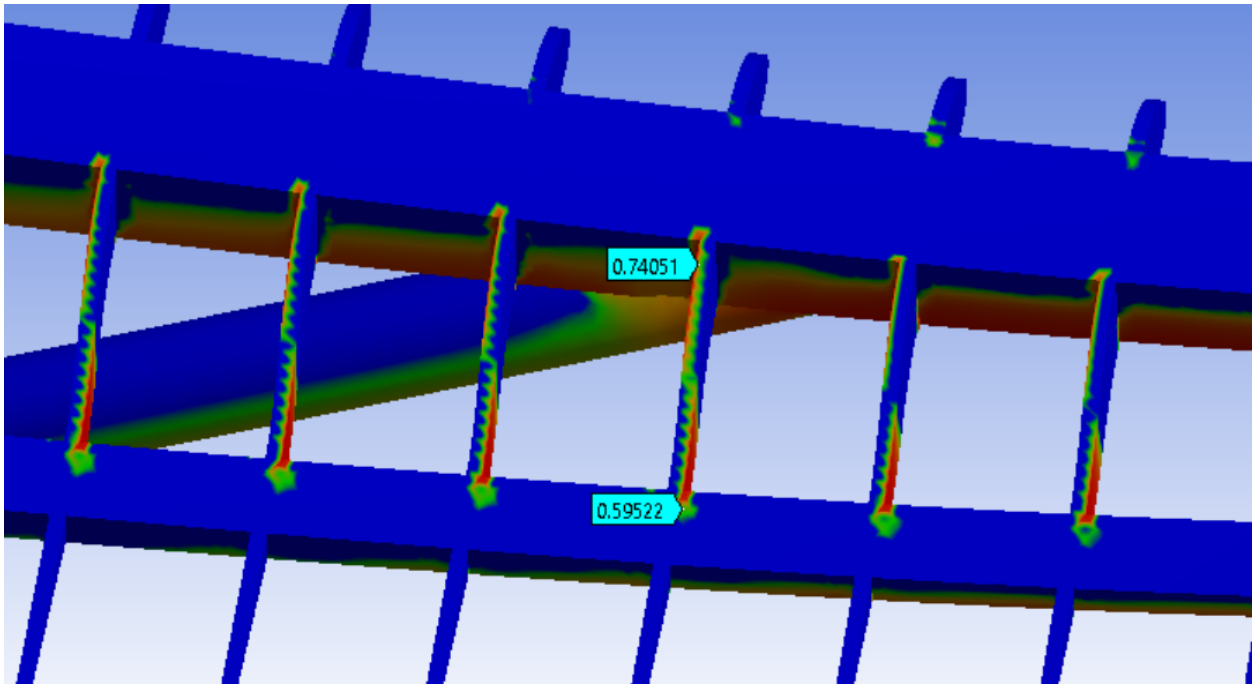

Figure 32 - Ribs shearing due to main and secondary spar moving in opposite directions

At a stress factor of safety of 0.82, the main spar is over stressed at the location outboard of the strut connection. To account for this, the strut will need to be positioned farther toward the wing tips to support the wing and reduce the tension. Based on the classical calculations, this will put more stress on the section between the wing strut connection and root, however based on the results of figure 34, that section of the wing has a FOS of 2.4 and can withstand more stress before hitting the design limit of 1.5.

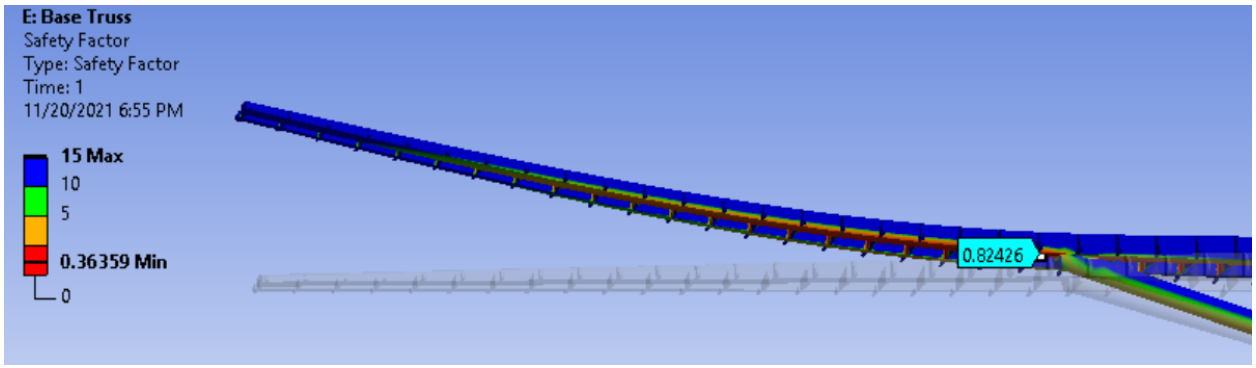

Figure 33 - Displacement outboard of the strut due to insufficient reinforcement on section

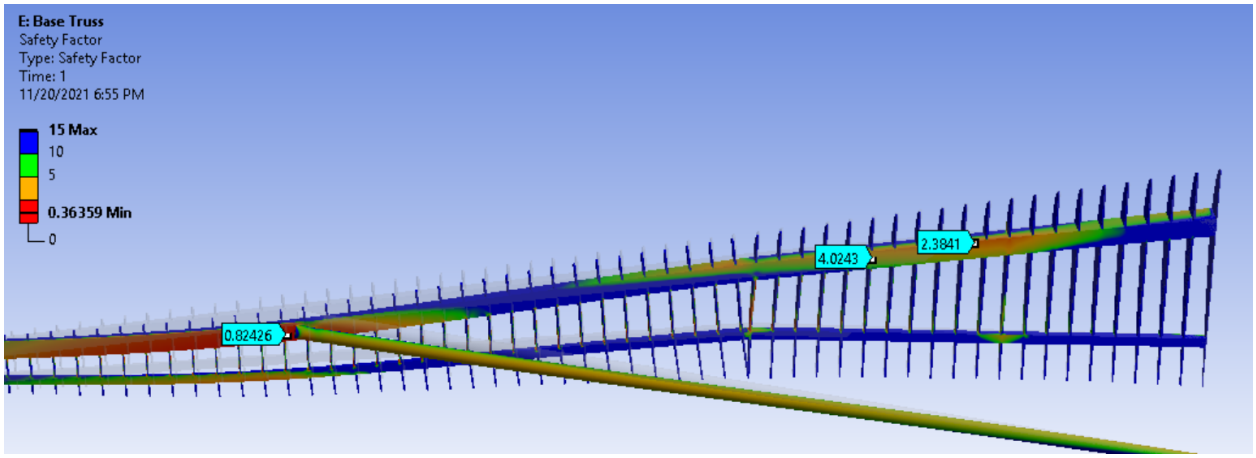

Figure 34 - Tensile stress has 0.82 FOS at strut joint while FOS at engine is 4

For the second iteration of design, the strut will be positioned in an angle more inline with the angle of wing sweep to prevent wing translation and load the strut only in the vertical direction.

In addition the strut will be connected to the wing in a farther outboard position to account for the high stress seen near the wing tips.

6.1.2 Strut Design Iteration 2

The next design iteration continues off the same wing geometry initially used in the first iteration however the strut connection to the fuselage is moved forward to a position 1.25m from the leading edge. Compared to the first design iteration, the point of the strut at the wing-strut joint translates significantly less in this design iteration. The translation in the reward direction is reduced from 0.48m to 0.1m. The net displacement of the wing at the strut's connection joint deflects 80% less than the previous iteration. Figure 35, shows the reduction in shearing force that this strut position change has had on the ribs.

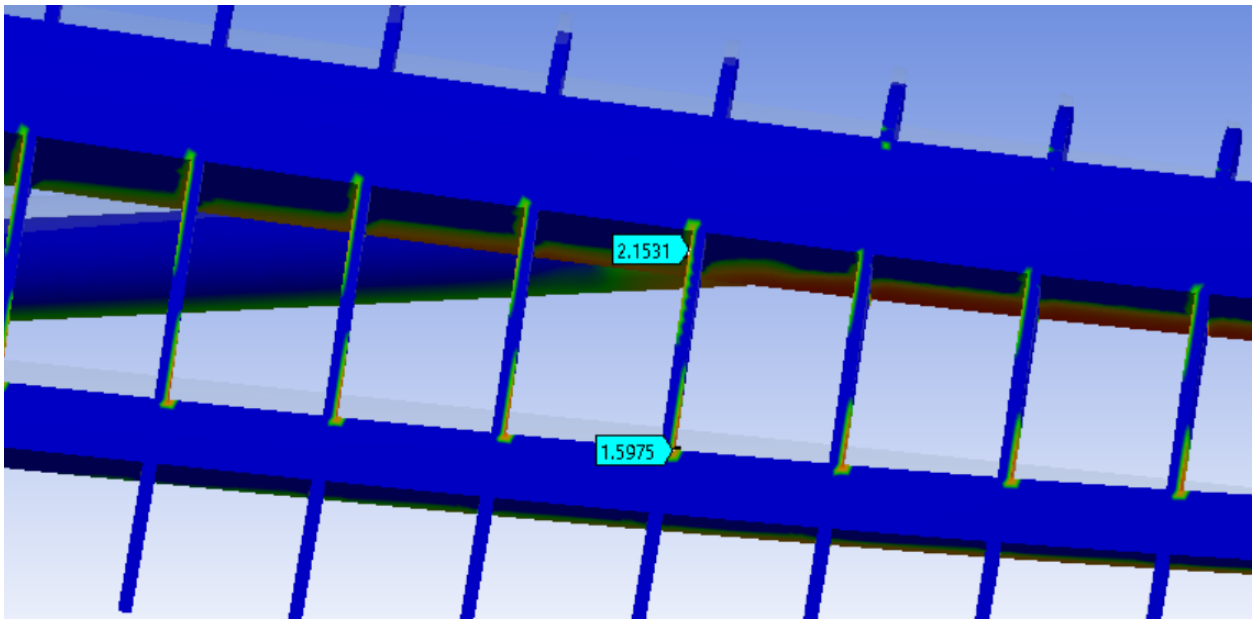

Figure 35 - Design change improves shearing force on ribs increasing stress FOS from 0.74 to 2.1

Repositioning the strut reduced the longitudinal translation of the wing. This has ultimately reduced the shearing stress seen on the ribs and reduced the deflection of the strut. The other improvement to be made is the peak stress seen outside of the strut connection. As

shown in the plot of figure 36 , repositioning the strut does not improve the high stress condition at the strut connection. The unsupported wing sectioned outside of the strut has enough lift to exceed the yield stress of the aluminium in the main spar at 260 MPa. Figure 37 shows that the mainspar is not stressed within the acceptable 1.5 factor of safety until 22.5 meters from the root or 2.5 meters from the joint.

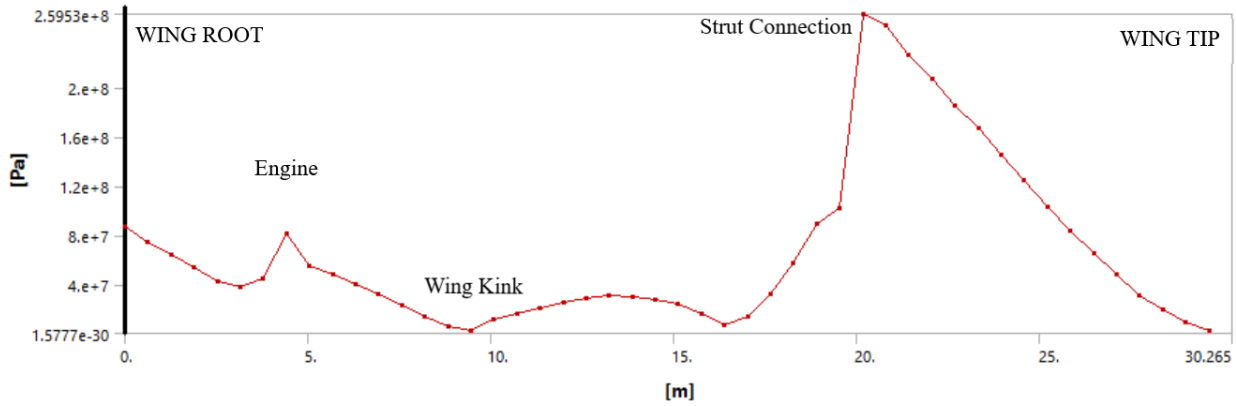

Figure 36 - Maximum principal stress along main spar of strut supported wing

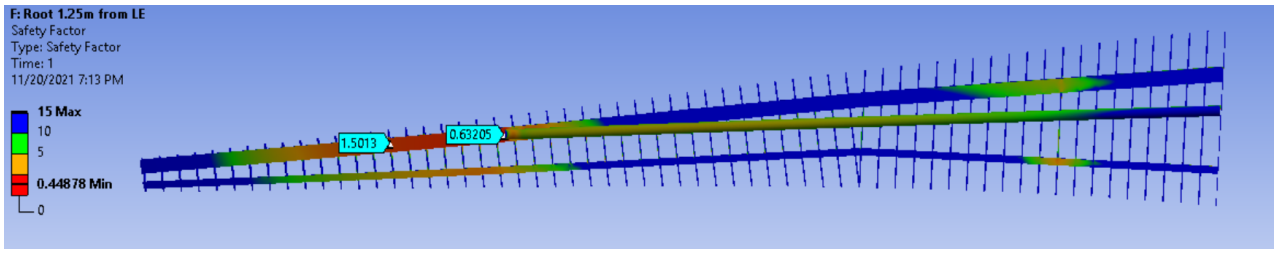

Figure 37- Stress FOS fails to meet 1.5 design specification between strut connection and 2m outboard

As stated in the previous subsection, to reduce the peak stress at the section outboard of the strut, the wing will be externally strengthened by extending the length of the strut to an anchor point on the spar closer to the wing tip. The stress sweeps from the classical calculations in Figure 15 of chapter 4 show a similar bending behavior for this cantilever section of the wing that has a more consistent chord length then the rest of the wing. Those calculations show that a strut move to a position 43% of the span results in 73% reduction in stress from the initial

cantilever wing. Being that the highest stress seen is 260MPa and needs to be reduced by 29% of that to 187MPa to achieve an acceptable 1.5 factor of safety, the strut will be moved so that the cantilever section is 17% that of the initial 10 meter free section. Moving the strut connection 1.7 meters outboard should allow the minimum stress to stay above the 1.5 factor of safety. Figure 38 shows the results of the study with a strut positioned at 22m from the root. The factor of safety is still below 1.5 minimum.

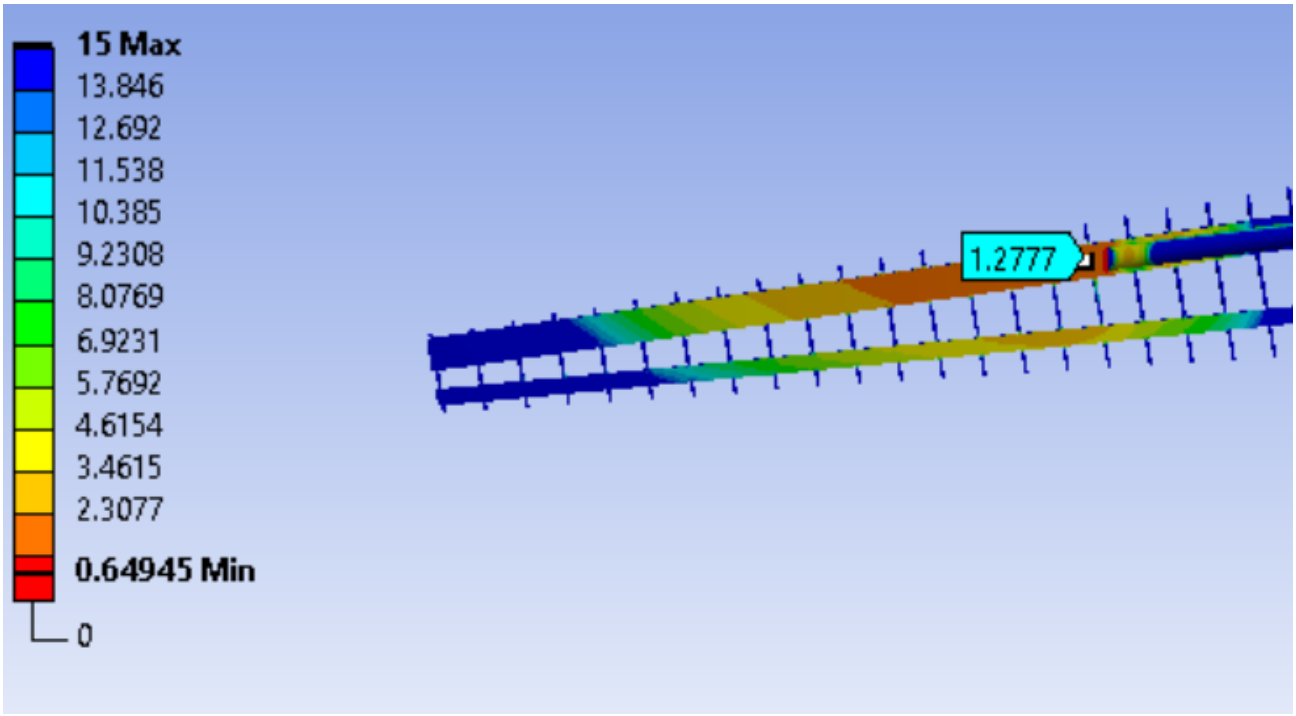

Figure 38 - Strut connected at 22m from root yields 1.28 Stress FOS

At 1.3, the strut needs to move outboard farther, and this improvement is shown in the figure 39 where the strut is positioned at 24 meters from the root. At that 24 meter position, the minimum factor of safety is now ~2 which is above the design parameters. Based on these two modifications, this second design iteration has solved both the high stress at the strut and ribs.

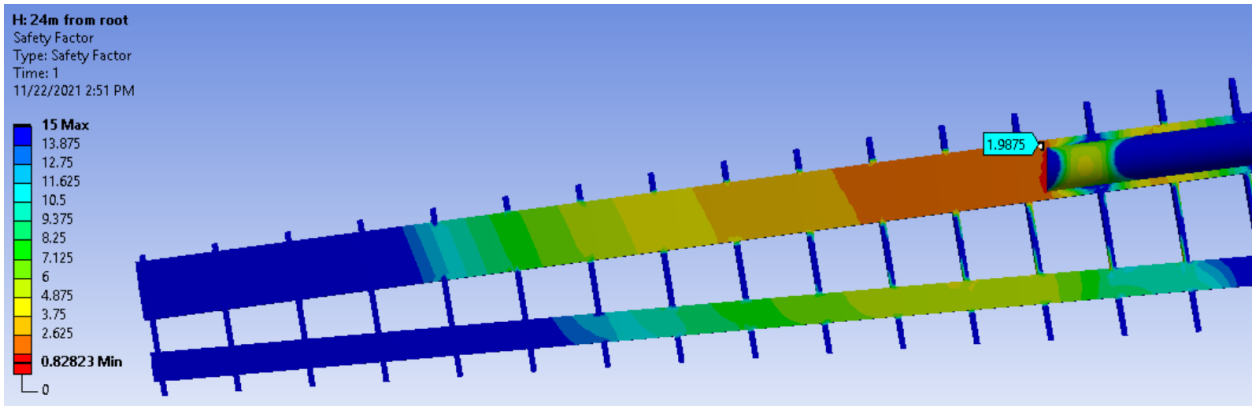

Figure 39 - Strut connected 24m from root results is stress within design specification

At the vertex or the connection between the strut and wing, there is an edge section of high stress. This is the only source of stress in the wing structure that is below the acceptable stress. As the stress propagation is confined to the strut joint itself and not distributed over a wider area, it is concluded that the root to this problem is from the connection itself. Figure 40 displays a 2.5x deformed model. As the wing deflects upward from the lifting load, the connection point twists and the strut deflects upward to account for this. Being that the strut is not under the direct load of the wing lift, the deflection upward is a result of the moment about the joint that twists the strut counterclockwise toward the wing tip. Reducing the moment on the joint will reduce the stress on the joint and result in a more acceptable joint. Iteration 3 covers this modification.

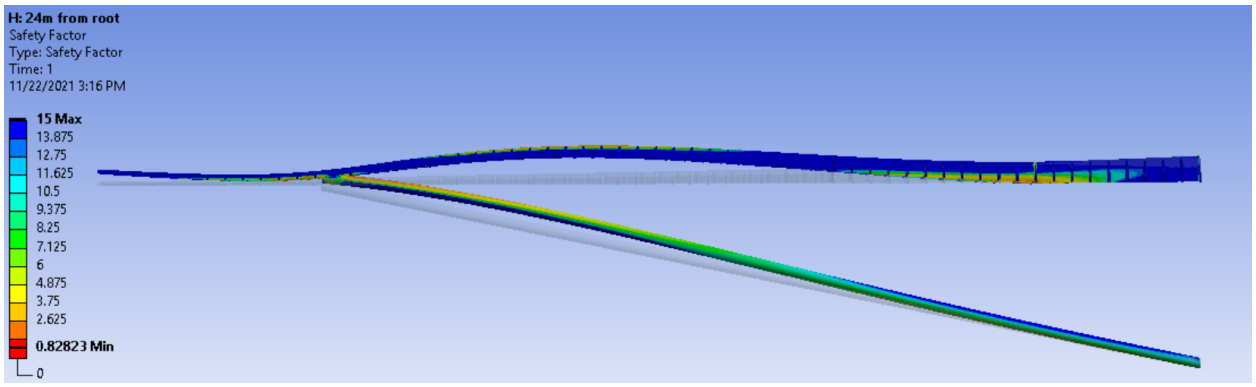

Figure 40 - 2.5x Deformed model of fixed strut configuration resulting in strut deflection as a result of wing deflection

6.1.3 Strut Design Iteration 3

As described in the previous subsection, the moment on the joint as a result of the lifting force from the wing causes high stress locations at the strut-wing joint. The stresses are exceptionally high at edges on the wing tip and root side of the strut connection, highlighted in figure 41, thus showing that the moment is bending the immediate connection between the strut and wing.

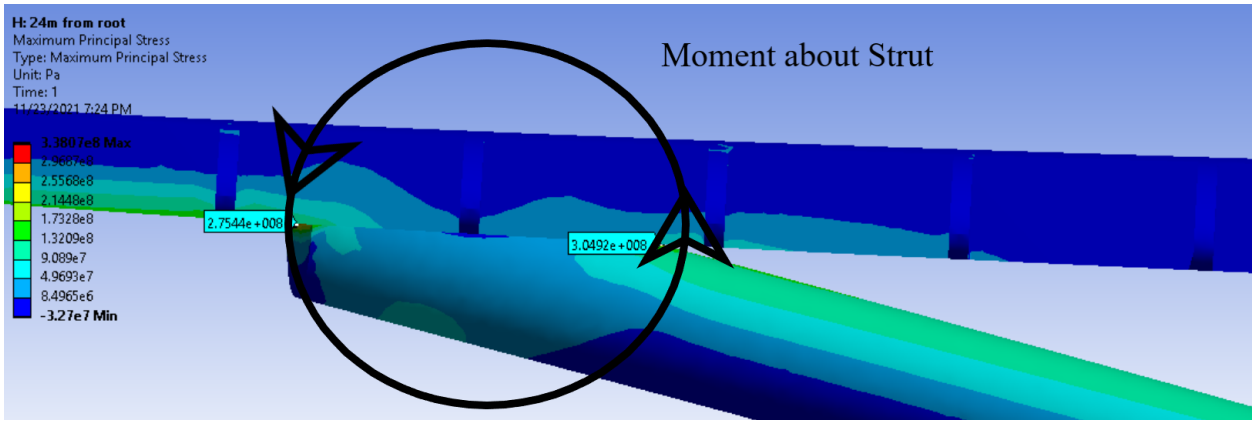

Figure 41 - Moment about strut connection causing high stress at edges

In this design iteration, a joint is used that removes this moment on the strut connection. Instead of a fixed joint, the strut and wing are separated into two bodies and connected by a pin joint to allow free rotation. In ANSYS, the bodies are inserted as an assembly and the pin is simulated as a revolute joint with one degree of rotational freedom.

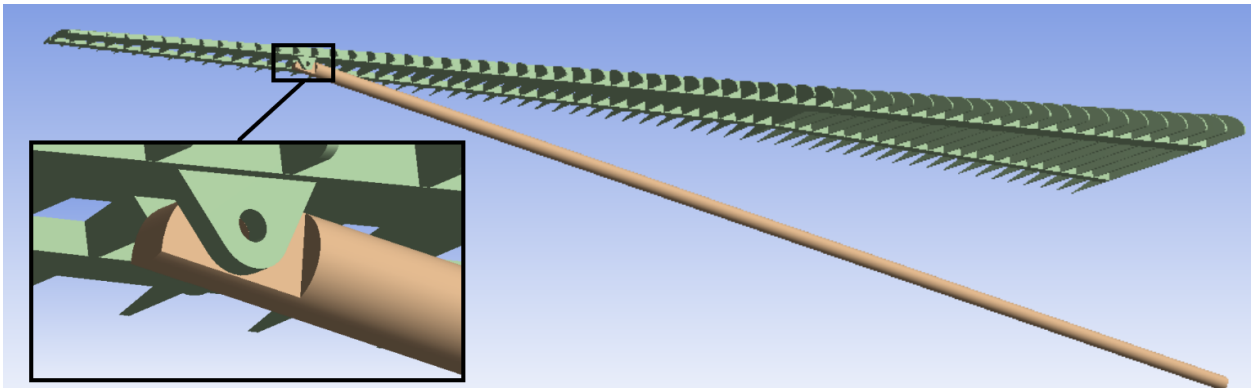

Figure 42 - Assembly of strut supported wing with pinned strut-wing connection

The addition of the pin joint reduced the maximum stress at the strut from 275MPa to 240MPa on the outboard section of the joint and from 304MPa to -3MPa on the inboard edge. As a result of the strut being mostly under tension as due to the pinned joint, the load direction from the strut that propagates through the wing bracket is seen in figure 43. This line of stress directly propagates through the edge of the bracket and results in the high stresses seen at the edges. A more optimized bracket is needed to disperse the load in the direction of the strut load.

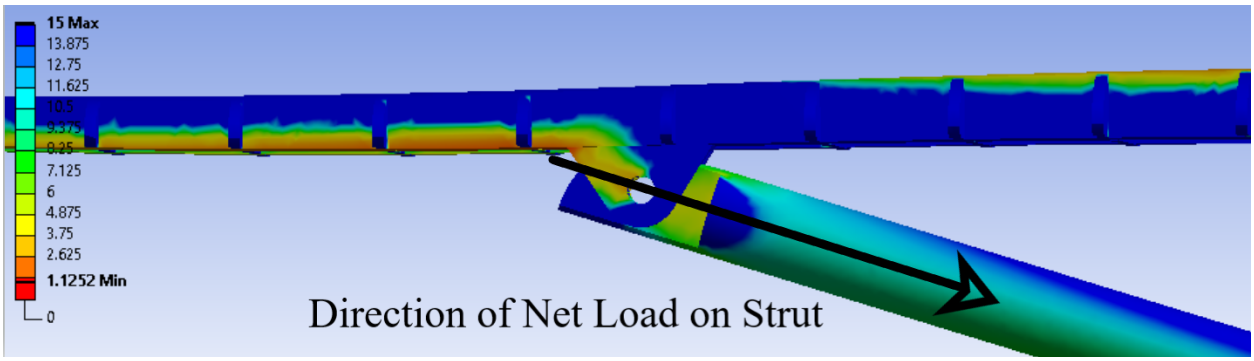

Figure 43 - FOS stress propagation on bracket follows direction of load from strut

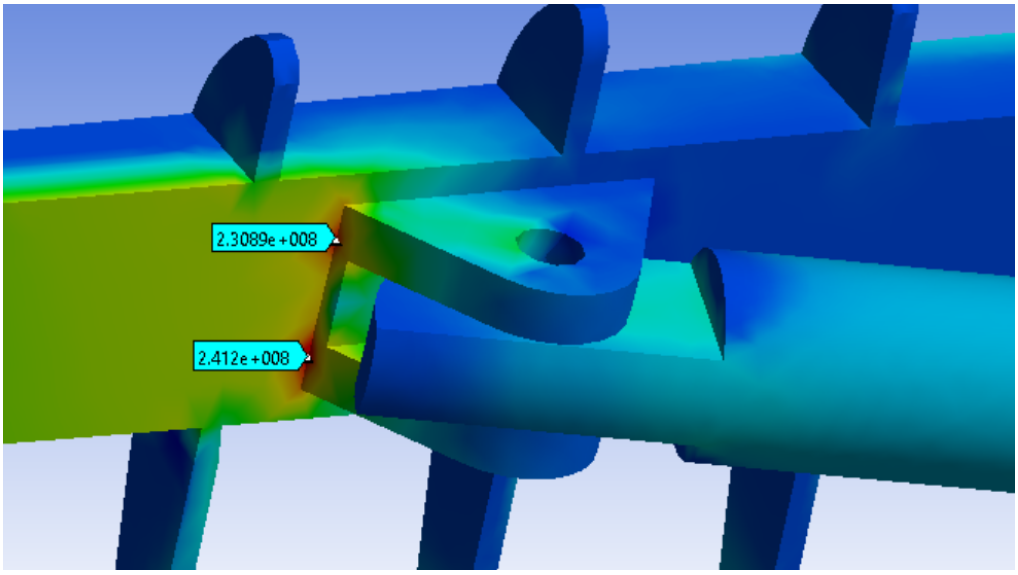

Figure 44 - Stress peaks seen at edges of pin bracket [pascals]

6.1.4 Strut Design Iteration 4

The fourth strut design iteration revolves around the stress observed about the immediate connection specifically on the edge between the bracket and the horizontal wing surface. A geometrical modification is done to the bracket by extending the amount of bracket material in the wing tip direction to account for the stress seen due to the load direction of the strut. A comparison between the two strut brackets in figure 45 and 46 shows the effect of this modification.

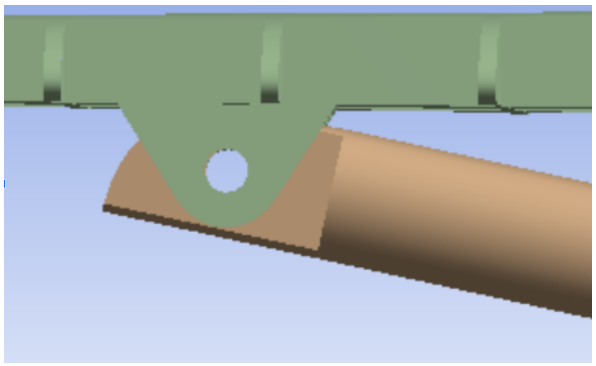

Figure 45 - Unmodified strut connection bracket

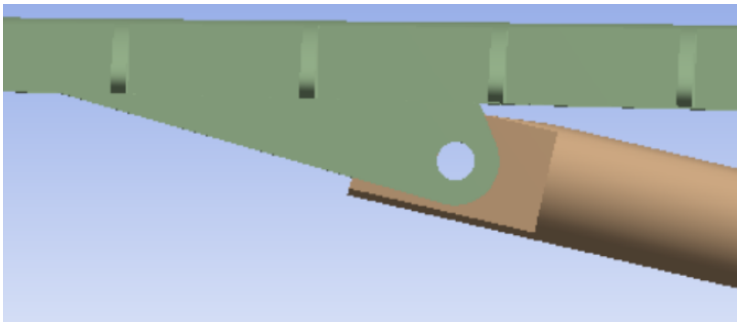

Figure 46 - Iteration 4 modified strut connection bracket

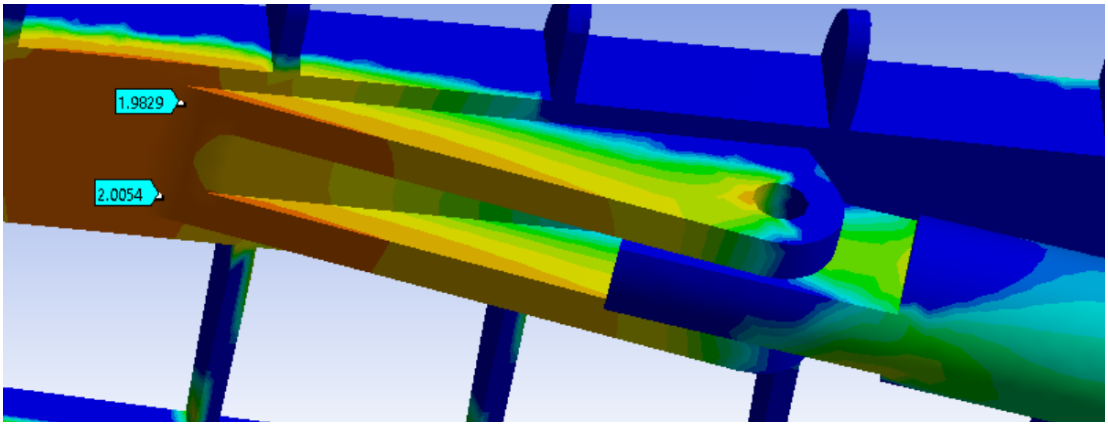

Figure 47 - Stress FOS at on modified bracket within stress parameters

The modification shows an improvement and reduction in the maximum stress seen at this bracket location. The minimum factor of safety for stress is reduced from 1.1 in the previous design iteration to ~2 which is within the 1.5 design limit.

6.1.5 Strut Design Iteration 5

After the design change in the previous chapter, the wing is constructed in a way that it can handle a 2.5G lifting load. It is expected for the wing to perform not only under lifting load but the loading of its own weight when on the ground. In this case the strut will be loaded in compression as it bears the load of the wing weight. The strut member as a part of the truss configuration will be strongest under tension, however under compression will be susceptible to buckling, which happens at a much lower load then that of tension. The critical buckling stress for the circular strut member is define as [19]

$$\sigma_{crit} = \pi^2 E(\frac{r}{L})^2 \quad (9)$$

where r is the radius of the circular cross section. The connection between the root and the strut is fixed while the connection between the strut and wing is pinned. Thus this pinned to fixed strut will have an effective length k = 0.7.

The wing loaded without the boundary condition of lift shows that the maximum stress occurs on the strut. A study sweeping the strut through various thicknesses between 0.3 meter and 0.15 meters diameter tracks the maximum principal stress that occurs through the strut. Figure 48 shows the results of this study.

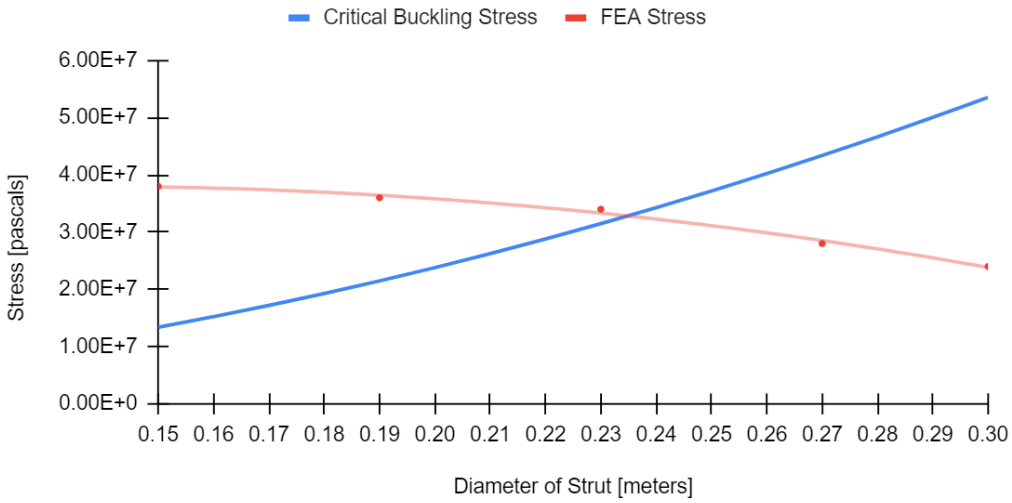

Figure 48 - Comparison between the calculated critical buckling stress compared to the FEA simulated maximum stress for each strut diameter

The blue line shows the calculated stress in which buckling will occur, while the red line shows the results from the FEA models at various diameters. As calculated by the red line, the maximum internal tensile stress in the strut reduces as the diameter of the strut increases. Similarly, the stress to induce buckling increases as the strut diameter increases. As shown in figure 48, increasing the strut thickness increases its ability to resist buckling. The intersection

between critical buckling stress and maximum stress at 0.235 meters is the resultant smallest diameter that the strut can be before it buckles under the weight of the wing.

6.2 Strut Design Overall Results and Additional Considerations

The three designs have corrected the main issues that have stemmed from the incorporation of the strut and made the strut a usable component. The condition that were accounted for include the following:

- Strut attachment point on spar is adjusted to a position farther outboard to reduce maximum stress on the wing section outboard of the connection
- Strut angle is adjusted to a position parallel to the direction of main spar sweep as to avoid translational movement in the wing and deflection in the strut
- Connection method between the strut and wing changed to adjust for moment reaction cause by wing
- Bracket design adjusted to account for direction of stress seen on bracket from strut loads
- Strut thickness is optimized to reduce the material to a function without buckling under wing load

The weight of the wing as a cantilever setup weighs 18352 kilograms and can not support itself without external bracing. The optimize bracing increases the weight of the assembly by 3154 kilograms. This is a necessary 17% increase in weight to support the wing.

7. Introduction of Jury Members in the Strut Braced Assembly

As discussed in the experiments run by the SUGAR project, the consideration of jury members has potential benefits to add to the strut setup. A jury member will connect the strut to an additional second point on the wing anchoring at a position some length along the strut. Chapter 6 studies run under a compressive load demonstrated that buckling was a limiting factor for the thickness of the strut. A jury in this chapter is run with the goal of reducing the maximum stress on the strut due to compressive loading and allow for a thinner strut to be used. A thin enough strut and jury assembly would be lighter than a strut alone and result in a lighter and less invasive bracing configuration.

7.1 Method of Jury Incorporation

The Jury configuration incorporates the strut section as discussed in chapter 6 as well as a vertical member connecting the midsection of the strut to the midsection of the wing. The base setup is shown in figure 49, in which a vertical jury is positioned at 17 meters from the wing root. To observe the effect of the jury anchoring to the wing in addition to the strut, all joints and connections are fixed.

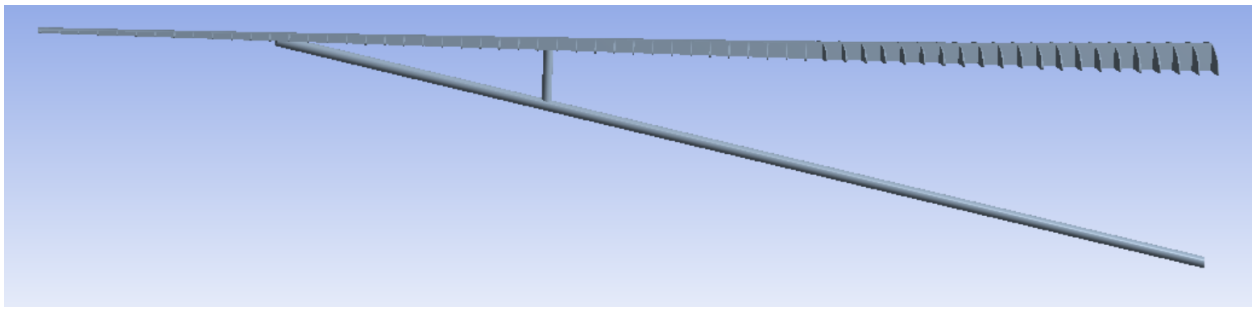

Figure 49 - Geometry of truss setup with vertical jury member at 17 meters from wing root

Figure 50, illustrates stress intensity, which is the absolute value of the maximum principal stress, so that both compressive and tensile stresses are seen. Comparing the stress along the

main spar between a fixed connection strut and fixed connection truss that incorporates a jury member, it is apparent that during the 2.5G lifting condition described in chapter 5, peak stress points at the engine and strut connection are nearly identical. This is due to the peak stress points being at fixed joint locations. The root of these stresses are due to direct moments about the joint and less about deformation in the wing itself. These peak stresses can only be reduced by changing the joint itself or the magnitude of geometrical bend in the wing. When comparing the maximum displacement at the jury member, the jury member has reduced vertical displacement from 0.3 meters to 0.1 meters. The largest improvement as a result of the jury member incorporation is seen in between the ~17 meter and ~23 meter distance from wing root. This is the section between the jury connection and strut connection. While the peak bending stress in the wing utilizing the individual strut is seen to be 0.13 GPa, the jury reduced it to 0.046 GPa.

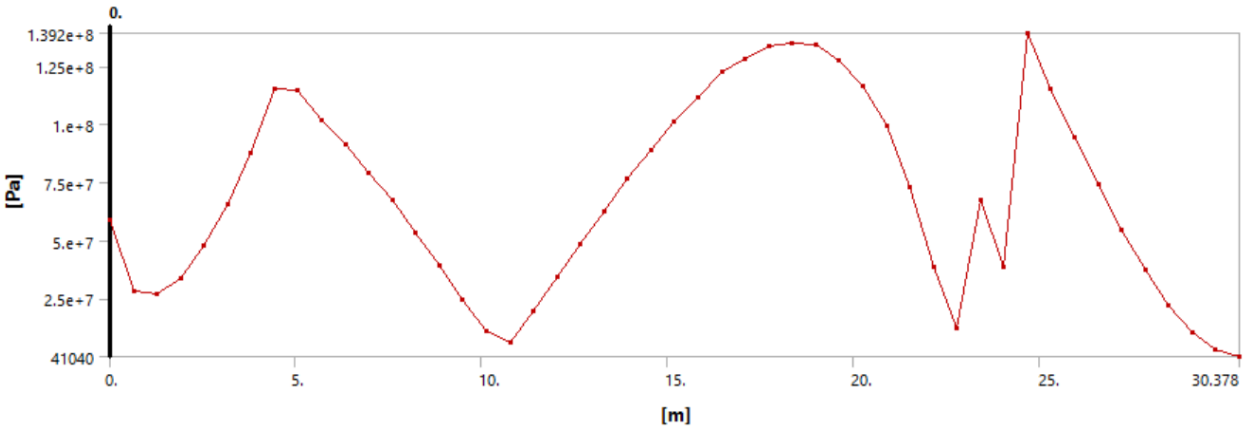

Figure 50 - Stress intensity along the main spar in a single strut configuration from wing root to tip

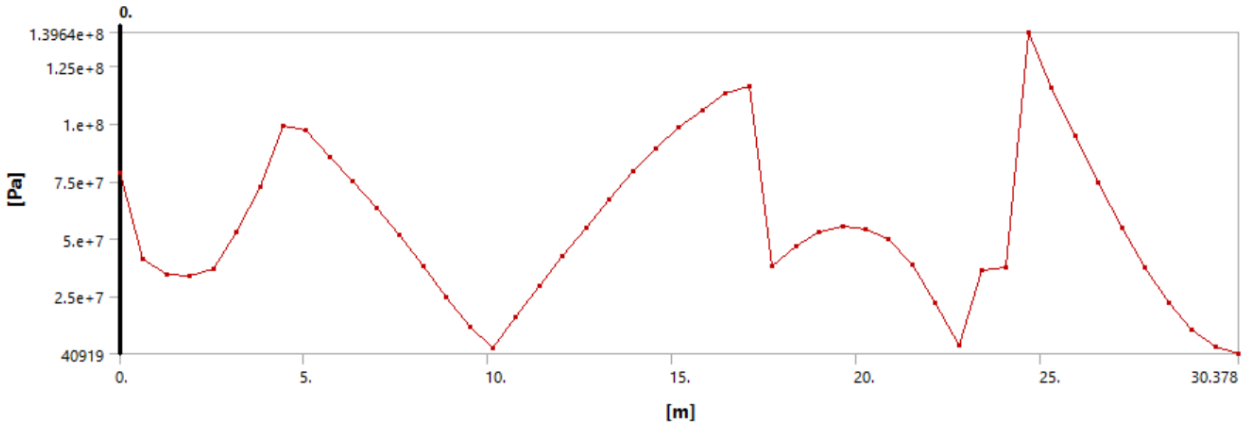

Figure 51 - Stress intensity along the main spar in with a single strut and vertical jury at 17 meters from wing root to tip

Between the engine and jury connection, the stress distribution is similar. This section does not act like a standard loaded beam fixed at both ends, and acts more in line with the distribution seen in the non jury setup in the section. Stress immediately drops at the jury location from its peak.

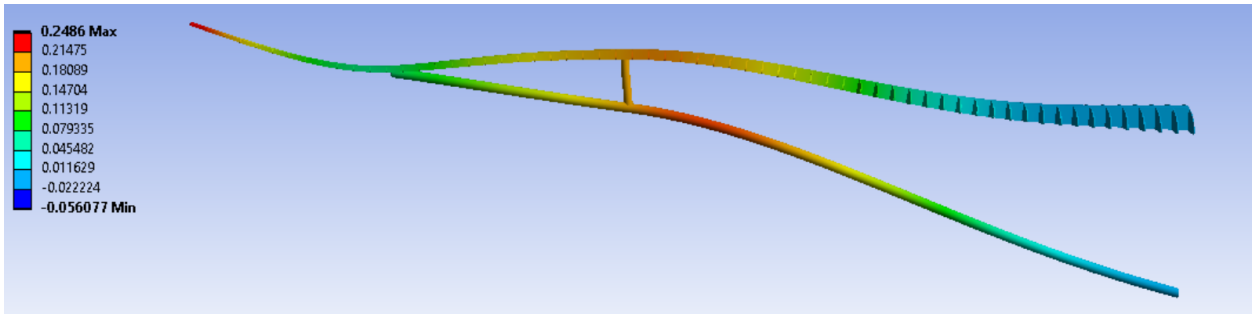

Figure 52 - 6.3x Deformed displacement contour of jury braced wing [meters]

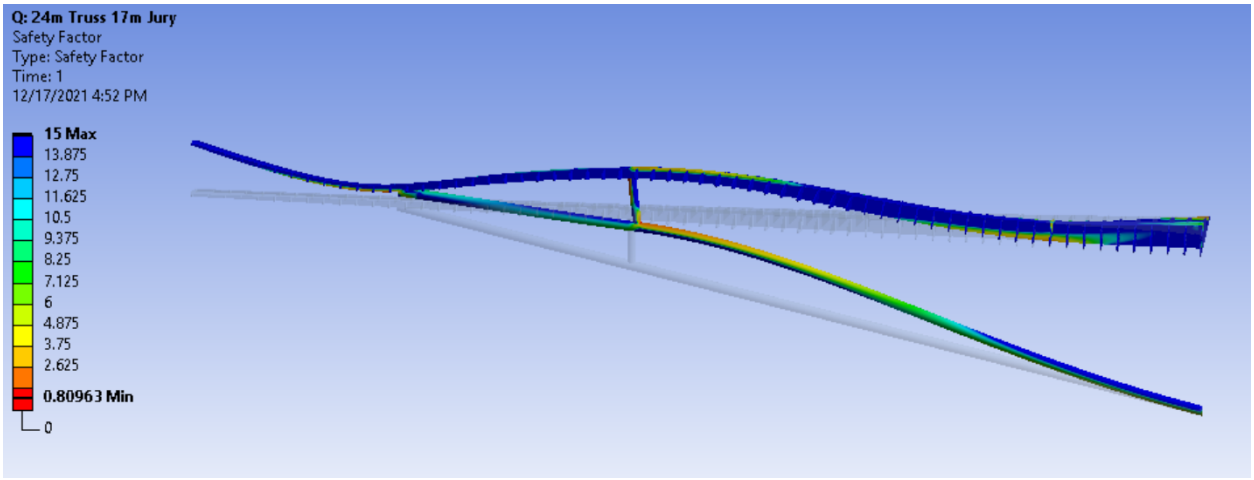

Figure 53 - 6.3x Deformed stress FOS contour of jury brace wing [pascals]

In this configuration, the wing is more strongly supported than the single strut setup, however the fixed connection between the jury and strut results in a high stress location on the strut that surpasses the yield strength of the aluminum. As a result, this reduces the effectiveness of the jury making it less practical than a single strut setup. Similar to the wing deflection in the previous strut configurations without a jury, maximum wing deflection is seen between the engine and the strut joint roughly where the jury connects to the wing. Figure 52 shows how this displacement is directly transferred to the strut which fails to resist its lateral load. Peak stress is seen at the joint between the strut and jury as the top of the jury translates upward with the wing's deformation pattern. The upward translation from the jury is what laterally deflects the strut and creates a high stress on the strut. Although the jury reduces the effective length of the strut, it also introduces a new load that deflects the sturt laterally which is preferable for a strut that should ideally be loaded longitudinally. A similar case run by NASA SUGAR project, the deflection seen at the joint between the strut and jury shows a similar result in which the jury pulls the strut into a state of lateral deflection. This is enough to determine that a vertical strut would not suffice for this lifting case and strut configuration.

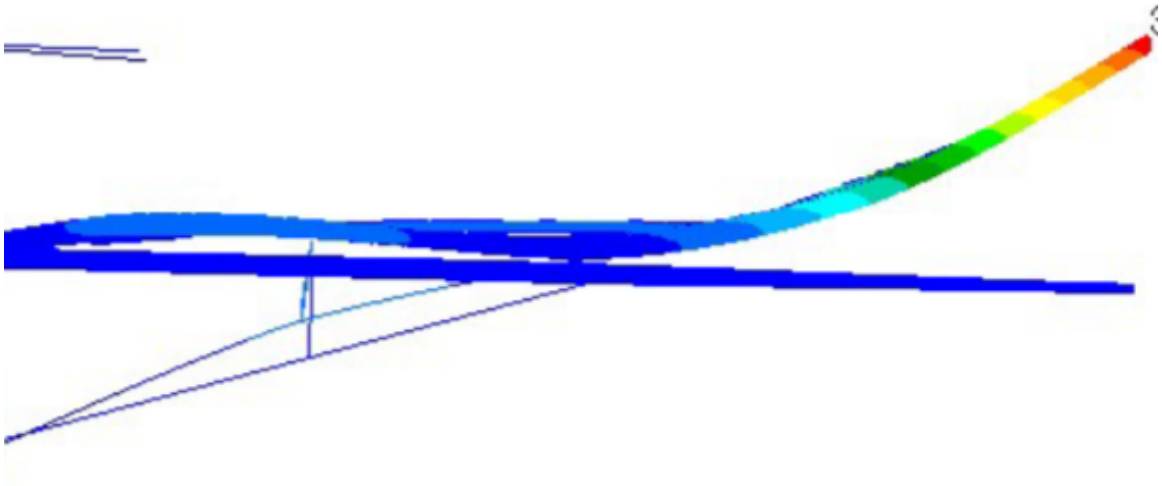

Figure 54 - Ultra Green aircraft jury braced model showing a similar high deflection at the strut to jury joint

7.2 Angled Jury Configuration For Strut Relief

The primary concern utilizing a jury is the introduction of lateral loading on the strut. Compared to pure tension, beams displace easily under lateral load and a method to lower this is required while still retaining benefits of a jury on the wing. In addition to the lateral load, the moment created by the jury on the strut increases the stress at the joint. To adjust the design, the jury is repositioned from perpendicular to the wing to an angle of 55 degrees.

The jury in the previous subsection created a moment about the strut to jury connection and by angling the jury, the moment on the connection is decreased. Figure 55 illustrates this concept.

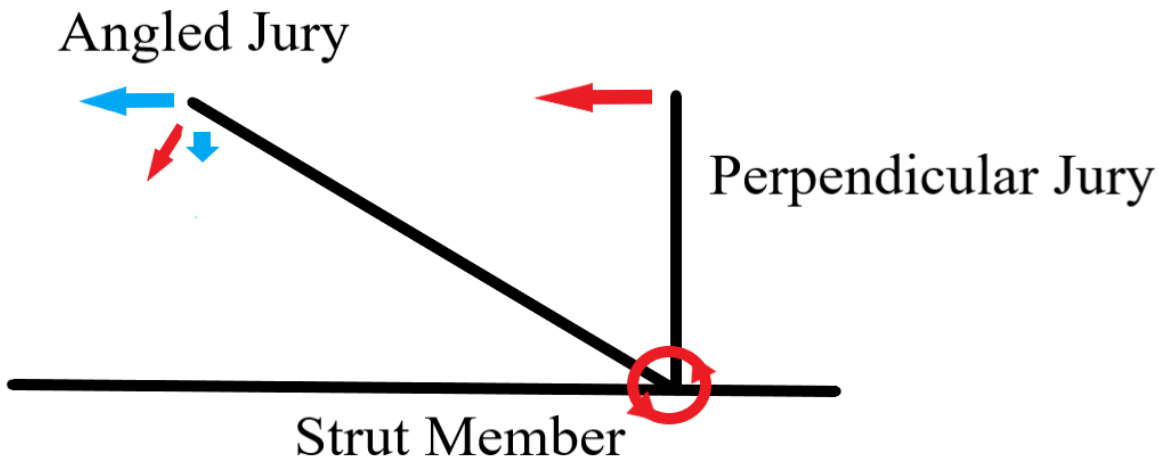

Figure 55 - A jury angles, the component contributing to moment about the joint decreases

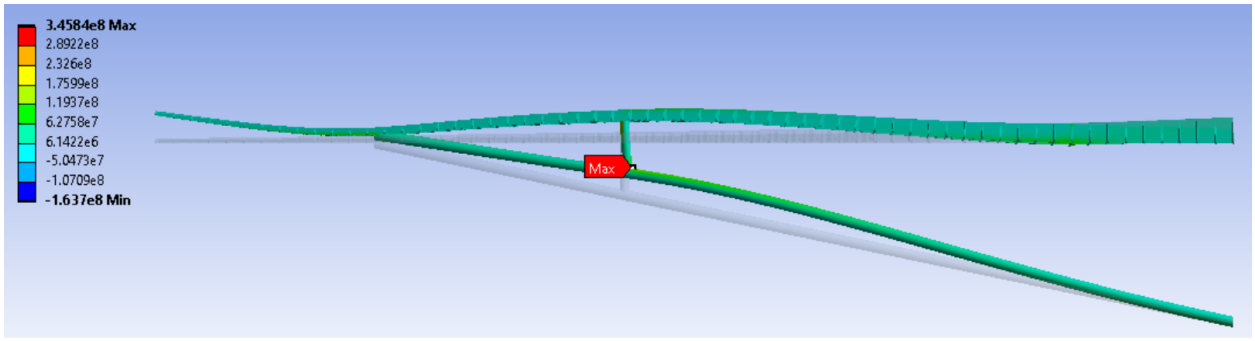

Figure 56 - Maximum stress on perpendicular connection is 3.46E8

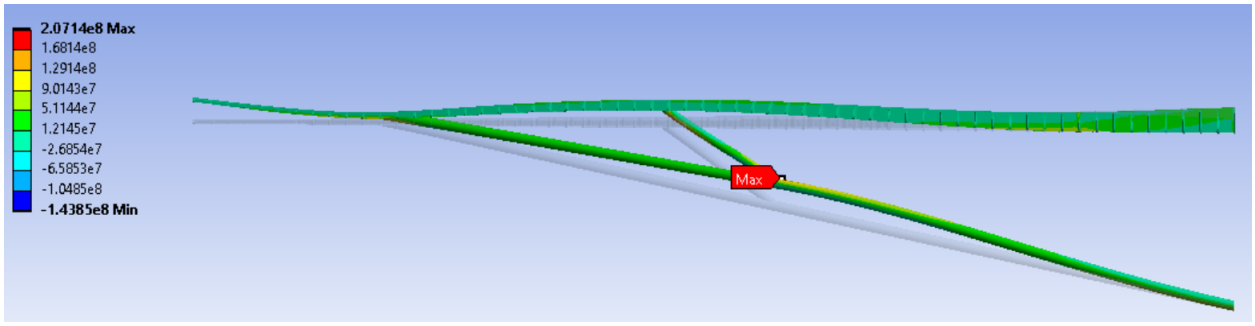

Figure 57 - Maximum stress on the connection is lowered to 2.01E8 pascals

The resultant change does improve but does not solve the condition. The effectiveness of this method lowers as the angle is increased as the closer the jury joint gets to the next strut joint, the less effective the jury is in preventing wing displacement and the heavier the external bracing mechanism gets. Under the lifting condition, the jury connection fails due to the moment and lateral load exerted on the strut. Utilizing the successful design with the strut, the assembly fails at the strut to jury joint. When the wing is allowed to move about the jury connection, there is additional wing displacement that puts more stress on the strut to jury connection.

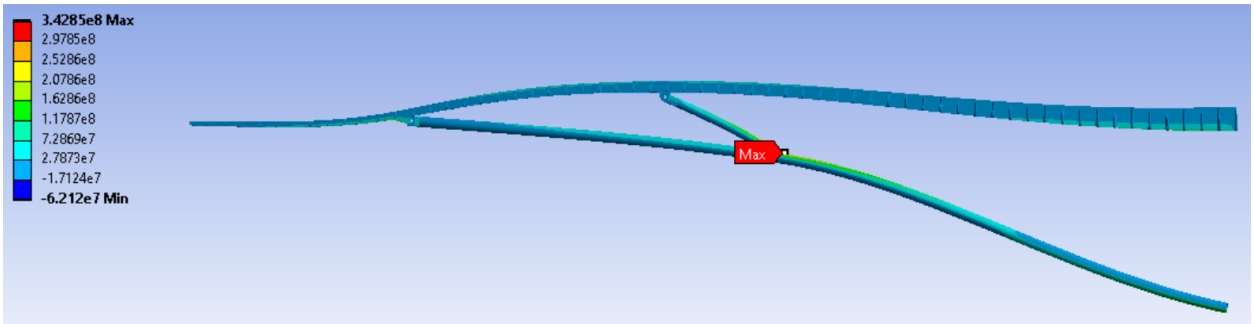

Figure 58 - Maximum principle stress with angled jury and pinned on all wing connections

7.3 Jury Connection Conclusion

The jury is initially considered to prevent strut from buckling downward under negative load. However the jury cannot operate under lifting loads without laterally loading the strut and buckling it upwards. In addition, a moment is caused by the strut as it translates creates a peak stress at the strut to jury joint resulting in an out of specification condition in which the aluminum material stresses past its yield point. So as a conclusion for the lifting case, a solid jury cannot be used. If the jury were used to prevent strut buckling in the downward direction, it would need to have no effect on the strut during position lift. This potentially could be done by utilizing a horizontally sliding mechanism at the strut - jury joint to allow for translation and shock or extending-jury that bottomed out at a specified distance. A sliding mechanism allows the wing jury to translate without causing a moment and the limiting extension would allow the jury to extend enough for the wing to displace without laterally loading the strut, but lock out

before the bend under negative load. This being, the complexity and number of exposed moving parts in this joint would most likely be too complex for an aerodynamic system especially operating in supersonic conditions.

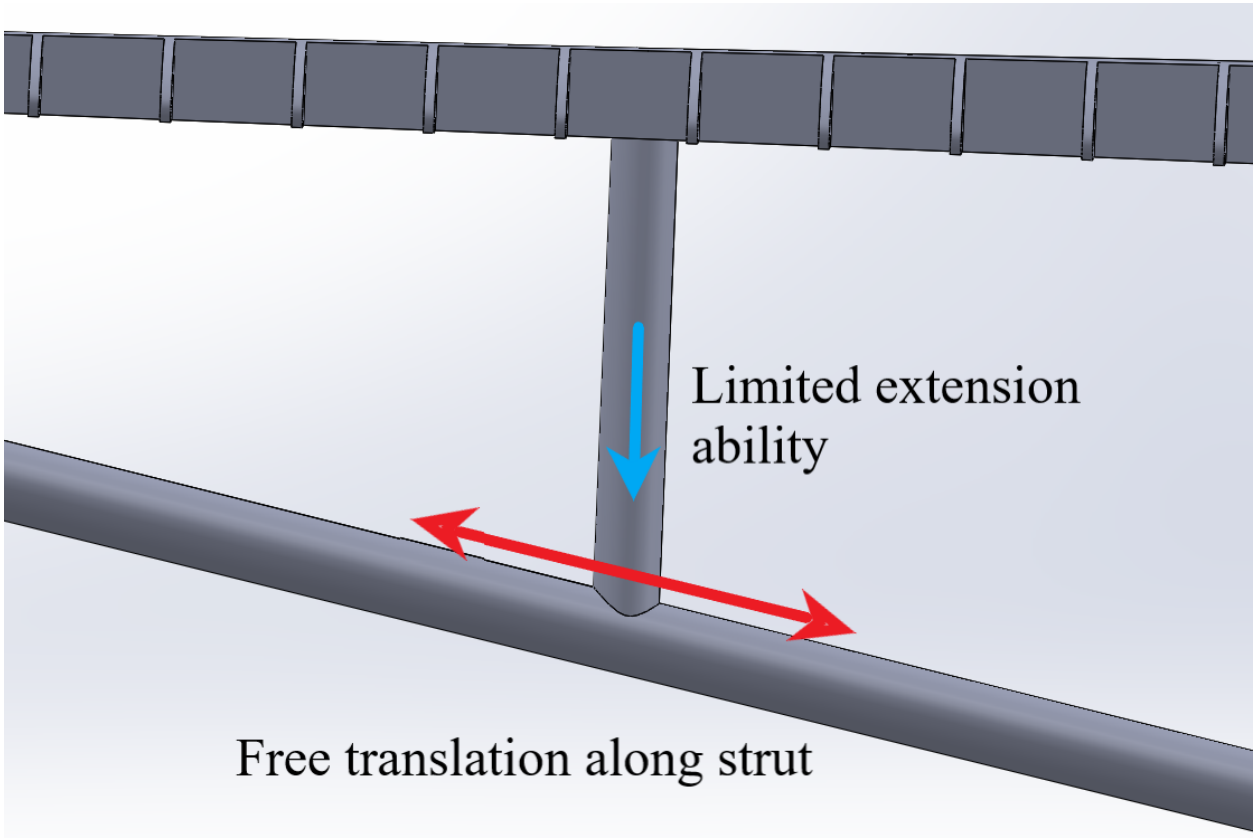

Figure 59 - Potentially feasible strut jury connection design

8. Conclusions, Results, and Future Work

This chapter points out the results and conclusions of the study done in this paper as well as calling out shortcomings in the designs that would require reconsideration before being applied to a full scale aircraft.

8.1 Conclusion and Results

During the duration of this study, the optimization and factors that affect the operation and performance of a high aspect ratio wing are analyzed. The two primary designs considered are a single strut braced design and a strut with jury members. With the base configuration, it is verified that the wing cannot hold itself up without external bracing. There is no way to internally brace a wing with the same aspect ratio of the SUGAR wing concept. A strut braced concept was proven to successfully support the wing under 1.5 FOS guidelines and under negative load. With a strut design, the strut needs to connect to the wing at a distance of ~80% of the span to prevent the wing tips from stressing past the point of material yield. The high aspect ratio causes deformation in the wing that is enough to damage the connection between strut and wing, thus the moment caused by the wing deformation needs to be accommodated through the use of a pin joint. When the wing performs under negative G's the strut has a tendency to buckle with the compressive load and lateral force of its own weight. For the geometry used, a 0.235 meter thick solid strut is the most optimal sized strut that will resist buckling under the compression of the wing weight while limiting the strut thickness. Jury members in the structural case are considered and found to reduce the allowable load of the strut before failure. Although a jury does result in less vertical displacement along the wing, the displacement improvement is only seen in the 7 meter section between the jury connection and strut connection while the other 76% of the wing deforms the same as a strut setup without a jury. Based on this study, the most optimal method of bracing such a high aspect ratio wing is to externally brace it with a single strut at 80% span with a pinned connection at the wing the strut connection.

8.2 Recommendations and Future Work

During the process of this study, the frame and ribbing of the wing are not modified past the initial baseline cantilever design. The framing design was based on a full size aircraft, however modifications made to the frame to allow its implementation into the high aspect ratio external shape affect the ability for the wing to store important mechanical features such as fuel tanks and control surfaces. These are features that affect the structural performance of the wing and need to be designed in parallel with the wing frame. This wing design is intended to operate within the transonic and supersonic speed ranges and the geometrical shape of the strut design is subpar. The strut can either be covered by a non structural hollow fairing or have a new hollow strut designed based on the loading conditions seen on the solid strut. The hollow strut would need to perform under the same conditions seen by the solid strut and have the pinned joint connect to the wing.

As previously stated, the aerodynamic effect of the externally braced design would require further optimization prior to its complete incorporation into the wing design. The cross section of the strut bars themselves need to be reshaped into a more aerodynamic geometry through the use of fairings or physical changes to the rod shape themselves. Between the cantilever and strut and jury design, the lift drops by 5.1% and drag increases by 230%. This means that in the worst case jury setup, the drag created by the truss was more than the drag created by the wing itself.

Wing Configuration	Lift [N] (180m/s)	Drag [N] (180m/s)
Cantilever	858724	55083
Strut	831153	130294
Strut and Jury	815902	181721

Figure 60 - Lift and drag values for each bracing configuration

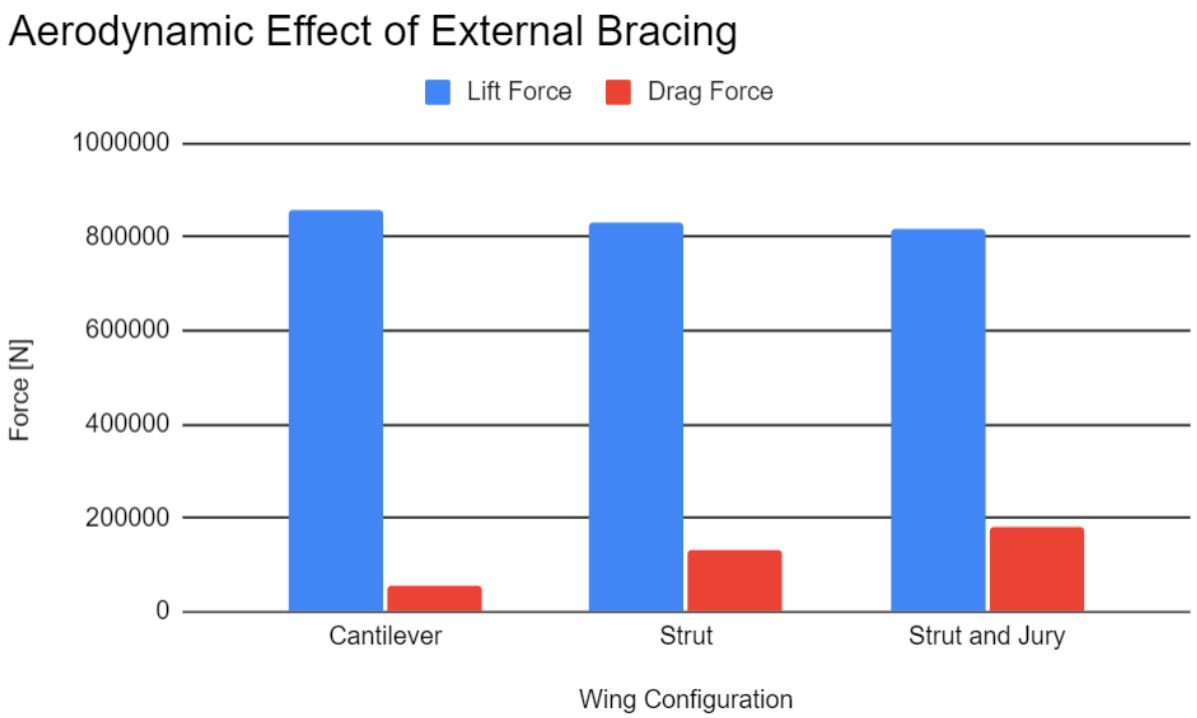

Figure 61 - Lift and drag value plot for each bracing configuration

References

[1] Bradley, M., and Droney, C., "How sweet the future of aviation," Boeing Available: https://www.boeing.com/features/innovation-quarterly/aug2017/feature-technical-sugar.page.

[2] Pfenninger, W., "Laminar Flow Control Laminarization," AGARD Rept. 654, Neully-sur-Seine, France, 1977.

[3] Gur, O., Bhatia, M., Schetz, J. A., Mason, W. H., Kapania, R. K., and Mavris, D. N., "Design Optimization of a Truss-Braced-Wing Transonic Transport Aircraft," *Journal of Aircraft*, vol. 47, 2010, pp. 1907–1917.

[4] *Bradley M., Droney C., "*Subsonic Ultra Green Aircraft Research: Phase I Final Report" NASA Report. April. 2011

[5] *Bradley M., Droney C., "*Subsonic Ultra Green Aircraft Research Phase II: N+4 Advanced Concept Development" NASA Report. May. 2012

[6] Chakraborty, I., Nam, T., Gross, J. R., Mavris, D. N., Schetz, J. A., and Kapania, R. K., "Comparative Assessment of Strut-Braced and Truss-Braced Wing Configurations Using Multidisciplinary Design Optimization," *Journal of Aircraft*, vol. 52, 2015, pp. 2009–2020.

[7] Kapania R., Professor M., Schetz J., Durham, F., Mallik W., Segee M., Gupta R., "Multidisciplinary Design Optimization and Cruise Mach Number Study of Truss-Braced Wing Aircraft," NASA Report. June. 2018

[8] Mallik, W., Kapania, R. K., and Schetz, J. A., "Effect of Flutter on the Multidisciplinary Design Optimization of Truss-Braced-Wing Aircraft," *Journal of Aircraft*, vol. 52, 2015, pp. 1858–1872.

[9] Wang, G., Zeng, J., Lee, J.-D., Du, X., and Shan, X., "Preliminary Design of a Truss-Braced Natural-Laminar-Flow Composite Wing via Aeroelastic Tailoring," ASDJournal, vol. 3, Sep. 2015.

[10] Wells, D. P., "Wing Configuration Impact on Design Optimums for a Subsonic Passenger Transport," 52nd Aerospace Sciences Meeting, 2014.

[11] Mansouri, R., “Structural analysis at aircraft conceptual design stage,” thesis, 2014.

[12] An automated CAD/CAE integration system for the parametric design of aircraft wing structures

[13] Anhalt, C., Monner, H. P., and Breitbach, E., “Interdisciplinary Wing Design – Structural Aspects,” *SAE Technical Paper Series*, 2003.

[14] Melber-Wilkending, S., and Wichmann, G., “Application of Advanced CFD Tools for High Reynolds Number Testing,” *47th AIAA Aerospace Sciences Meeting including The New Horizons Forum and Aerospace Exposition*, 2009.

[15] Barreda, V., “Conceptual Design Optimization of a Strut Braced Wing Aircraft,” thesis, 2013.

[16] Anderson, J. D., *Fundamentals of aerodynamics*, London: Mcgraw-hill Publishing Co., 2007.

[17] Bruhn, E. F., and Bollard, R. J. H., *Analysis and design of flight vehicle structures*, Carmel: Jacobs, 1973.

[18] Bristow, J. W., and Irving, P. E., “Safety factors in civil aircraft design requirements,” *Engineering Failure Analysis*, vol. 14, Apr. 2007, pp. 459–470.

[19] Holmes, D. P., Barve, S., Guerra, A., and Lautzenhiser, C., “Mechanics of materials: Beam buckling " mechanics of slender structures: Boston University,” *Mechanics of Slender Structures RSS* Available: https://www.bu.edu/moss/mechanics-of-materials-beam-buckling/.